Forced Oceanic Waves

S. G. H. PHILANDER

Geophysical Fluid Dynamics Program, Princeton University, Princeton, New Jersey 08540

This paper concerns the linear response of the ocean to forcing at a specified frequency and wave number in the absence of mean currents. It discusses the details of the forcing function, the general properties of the equations of motion, and possible simplifications of these equations. Two representations for the oceanic response to forcing are described in detail. One solution is in terms of the normal modes of the ocean. The vertical structure of these modes corresponds to that of the barotropic and baroclinic modes; their latitudinal structure corresponds to that of inertia-gravity and Rossby waves. These waves are eigenfunctions of Laplace's tidal equations (LTE) with the frequency as eigenvalue. The description in terms of vertically standing modes is particularly useful if the forcing is nonlocal, because only these modes can propagate into undisturbed regions. The principal result is that it is extremely difficult for baroclinic (but not barotropic) disturbances to propagate horizontally away from a forced region. Instabilities of the Gulf Stream excite disturbances that are confined to the immediate neighborhood of the current; disturbances due to instabilities of equatorial currents do not propagate far latitudinally. A second representation of the oceanic response to forcing is in terms of vertically propagating, or vertically trapped, latitudinal modes. These modes are eigenfunctions of LTE with the equivalent depth h (not the frequency) as eigenvalue. Both positive and negative eigenvalues h are necessary for completeness. The modes with $h > 0$ consist of an infinite set of inertia-gravity waves and a finite set of Rossby waves which either propagate vertically or form vertically standing modes. The latitudinally gravest modes are equatorially trapped and have been observed in the Atlantic and Pacific oceans. The modes with $h < 0$ are necessary to describe the oceanic response to nonresonant forcing. In the vertical this response attenuates with increasing distance from the forcing region. Because of the shallowness of the ocean the large eastward traveling atmospheric cyclones in mid-latitudes and high latitudes force a response down to the ocean floor. Interaction with the bottom topography will result in smaller-scale disturbances and will affect the frequency spectrum of the response when bottom-trapped waves are excited.

CONTENTS

A. INTRODUCTION

Practically all oceanic motion is in (direct or indirect) response to atmospheric forcing. In the past, interest has centered on the excitation of waves with inertial and shorter periods on the one hand and on the generation of nearly steady oceanic currents on the other hand. Recently, attention has focused on the frequency band between these extremes primarily because of the discovery of energetic 'eddies,' in this frequency band, in various parts of the oceans. Since the atmosphere forces the ocean at all frequencies, particularly subinertial frequencies (see Figure 1 and *Byshev and Invanov* [1969]), it is of importance to know to what extent these oceanic transients are atmospherically forced. In this paper we investigate the response of the ocean to forcing at different frequencies and wave numbers by reexamining the theory of linear waves in a stratified rotating thin spherical shell of fluid.

The oceanic response to forcing is usually described in terms of the natural modes of the ocean: standing baroclinic modes and the barotropic mode for the vertical structure and inertia-gravity and Rossby (planetary) waves for the horizontal structure. These modes can be used to describe the oceanic response to (nearly) any forcing because they form a complete set. Whether this representation of the solution is a convenient and useful one depends on the nature of the forcing. For example, this representation readily provides information concerning the propagation of energy away from a localized forced region. This is so because the natural modes of oscillation satisfy the unforced equations of motion. The description in terms of the natural modes is also valuable when these modes play a central role in the adjustment of the ocean from one steady state to another. Rossby waves play such a role when there is a sudden change in the intensity of the (otherwise) steady winds that drive the oceanic circulation. Except for the external mode these waves travel so slowly in mid-latitudes and high latitudes that it takes them several years to propagate across an ocean basin. It follows that the time scale for the baroclinic adjustment of the North Atlantic Ocean to a sudden change in wind conditions is of the order of decades [*Veronis and Stommel,* 1956]. In low latitudes, on the other hand, planetary waves travel much more rapidly, so equatorial oceans take of the order of weeks to adjust to a change in the winds [*Lighthill,* 1969]. These considerations are particularly relevant to the northwestern part of the Indian Ocean. There the onset of the monsoons can often be described as a sudden change from one nearly steady state to another nearly steady state [*Fieux and Stommel,* 1977]. Elsewhere, however, the ocean is forced continuously over a range of spatial and temporal scales. The precise range of these scales determines whether or not the

Paper number 7R0826.
0034-6853/78/017R-0826$06.00

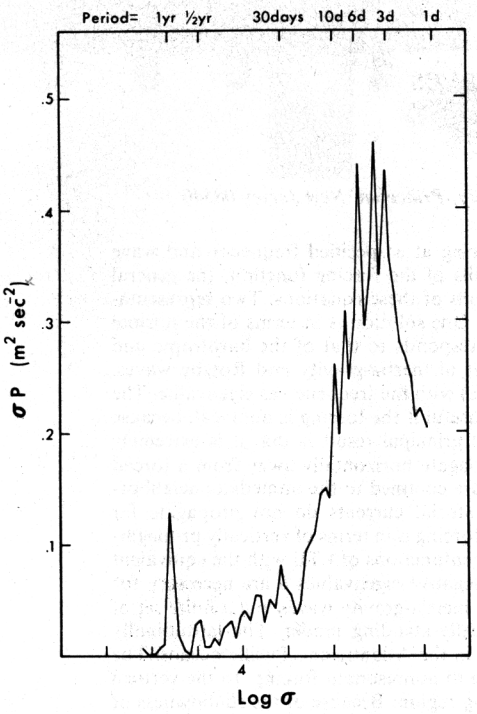

Fig. 1. Frequency spectrum of the surface winds at Caribou, Maine (47°N, 68°W). This spectrum is typical for latitudes poleward of 40°. Energy in the 2- to 10-day band is due to eastward traveling cyclones [after *Oort and Taylor*, 1969].

natural modes are important in the oceanic response and therefore whether or not a description in terms of these modes is useful.

Rossby waves are excited directly in the ocean only if the frequency–wave number range of the forcing function coincides with the shaded part of Figure 2. A recent analysis of the surface winds by *Willebrand* [1977] has shown that the most

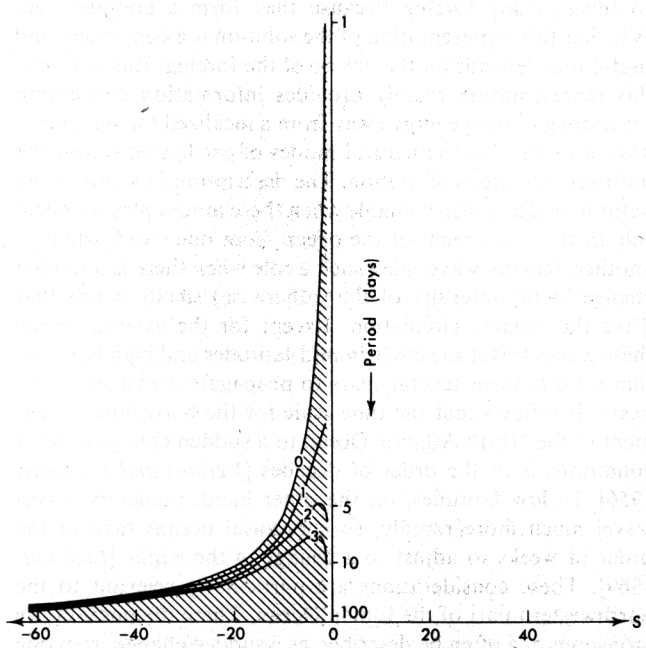

Fig. 2. The shaded region shows the frequency–zonal wave number range where Rossby waves are possible. The solid lines correspond to the four gravest meridional modes which have the highest frequencies (for a given s), according to (B9). Free Rossby waves, which can propagate away from a localized disturbance, have much lower frequencies for a given s (see section E).

energetic fluctuations of the winds are associated with large eastward traveling cyclones. These disturbances, which have time scales of from 2 to 10 days, force the ocean in the right-hand (unshaded) part of Figure 2. Measurements that show a correlation between fluctuations of oceanic currents and local atmospheric storms [J. Meincke, unpublished manuscript, 1975; *Taylor et al.*, 1977; *Baker et al.*, 1977] indicate that the response to such storms can be large. Further indirect evidence of forced (as opposed to freely propagating) oceanic waves comes from measurements of the kinetic energy spectrum in the oceans. The spectra all have a peak at the inertial period. At slightly lower frequencies, energy levels (below the surface layers of the ocean) drop sharply, whereafter there is an increase in energy levels as the frequency decreases further. This feature of the spectra is consistent with the presence of forced waves (which have amplitudes that decay exponentially in the vertical) at subinertial frequencies (see section H). It will clearly be of value to have a description of the oceanic response in which it is explicit that in certain frequency ranges, no freely propagating waves are excited. Section D of this paper contains such a description. It is complementary, and not necessarily preferable, to the description in terms of the natural modes of oscillation.

We have indicated that a description in which the existence of vertically standing baroclinic modes is not assumed may be useful in mid-latitudes and high latitudes. Such a description is also useful in the tropics. *Tyabin and Sleptsov-Shevlevich* [1975] find that the oceanic response to atmospheric disturbances coming off northwest Africa is trapped above the thermocline. Observations of equatorially trapped waves in the Atlantic [*Weisberg et al.*, 1977] show that they are downward propagating, not vertically standing, modes. In the Pacific Ocean, on the other hand, *Wunsch and Gill* [1976] have argued that peaks in sea level spectra correspond to resonant, first baroclinic mode equatorially trapped waves. This leads us to investigate the factors that can prevent the establishment of standing baroclinic modes.

This paper is organized as follows: The equations of motion and different methods for their solution are outlined in section B; in section C, which concerns the forcing function, it is pointed out that at low frequencies the curl of the wind stress is the only important term but at higher frequencies there are additional terms; in sections D and E the equations of motion are solved in two different but complementary ways; sections F and G concern the effects of coastal boundaries and of bottom topography, respectively; the implications of the various results are presented in section H; some of the limitations of the linear theory presented here are described in section I; and section J summarizes the principal results. Appendix B has a discussion of approximations to Laplace's tidal equations.

B. Equations of Motion

We consider linear waves in a rotating stratified spherical shell of fluid in which there are no mean currents. It is assumed that the motion is described by the following equations:

$$\frac{\partial u}{\partial t} - 2\Omega v \cos\theta + \frac{1}{a\rho_0 \sin\theta}\frac{\partial p}{\partial \phi} = \frac{\tau^x}{\rho_0 D} \tag{1a}$$

$$\frac{\partial v}{\partial t} + 2\Omega u \cos\theta - \frac{1}{a\rho_0}\frac{\partial p}{\partial \theta} = \frac{\tau^y}{\rho_0 D} \tag{1b}$$

$$\rho g + \frac{\partial p}{\partial z} = 0 \tag{1c}$$

$$\frac{1}{\sin\theta}\frac{\partial u}{\partial \phi} - \frac{1}{\sin\theta}\frac{\partial}{\partial\theta}(v\sin\theta) + a\frac{\partial w}{\partial z} = 0 \qquad (1d)$$

$$\rho_t + w\bar{\rho}_z = 0 \qquad (1e)$$

Here

$$\text{density} = \rho_0 + \bar{\rho}(z) + \rho(\theta, \phi, z, t)$$

$$\text{pressure} = -\rho_0 gz - \int \bar{\rho} g\, dz + p(\theta, \phi, z, t)$$

and the various symbols are as defined in the notation list. The wind stress $\tau(z)$, which has eastward and northward components τ^x and τ^y, respectively, is regarded as a body force in a mixed surface layer of depth D and is identically zero below that layer. The boundary conditions are the following:

Ocean floor

$$w = 0 \quad \text{at} \quad z = -H \qquad (2a)$$

Ocean surface

$$-\rho_0 gw + P_t = PA_t \quad \text{at} \quad z = 0 \qquad (2b)$$

where PA is an imposed atmospheric pressure fluctuation. We also require that the solutions be bounded at the poles ($\theta = 0, \pi$) or that the meridional velocity component vanish at coasts along circles of latitude.

Miles [1974] discusses in detail the conditions under which equations (1) are valid. These equations, together with the above boundary conditions, apparently constitute an ill-posed problem for certain ranges of the frequency σ of the motion. This is fortunately not so when

$$\sigma < 2\Omega \ll N$$

which is the range of parameters that interests us.

Assume solutions of the form $e^{i(s\phi - \sigma t)}$, where the frequency σ is always positive and the zonal wave number s is positive (negative) for eastward (westward) propagating waves. Equations (1) can now be reduced to the single equation

$$L(P) + 4\Omega^2 a^2 \frac{\partial}{\partial z}\left(\frac{1}{N^2}\frac{\partial P}{\partial z}\right) = F_1 \qquad (3)$$

where F_1 is the forcing function and

$$L \equiv \frac{1}{\lambda \sin\theta}\left\{\frac{\partial}{\partial\theta}\left[\frac{1}{\lambda^2 - \cos^2\theta}\left(s\cos\theta - \lambda\sin\theta\frac{\partial}{\partial\theta}\right)\right] + \frac{s}{\lambda^2 - \cos^2\theta}\left(\frac{\lambda s}{\sin\theta} - \cos\theta\frac{\partial}{\partial\theta}\right)\right\}$$

If we make the β plane approximations (see Appendix B), then a single equation for the meridional velocity component can readily be derived:

$$V_{yy} + (f^2 - \sigma^2)\frac{\partial}{\partial z}\left(\frac{1}{N^2}\frac{\partial v}{\partial z}\right) - \left(k^2 + \beta\frac{k}{\sigma}\right)v = -\frac{iF_2}{\sigma} \qquad (4)$$

a. Properties of the governing equations. These properties are as follows:

1. Between the circles of latitude given by $\cos\theta < \sigma/2\Omega$ the set of equations (1) is hyperbolic. The characteristics can be expressed in terms of elliptic integrals [*Miles*, 1974]. The approximate expressions for the two families of characteristics on an equatorial β plane are

$$\frac{y}{2}\left(\sigma^2 - \beta^2 y^2\right)^{1/2} + \frac{\sigma^2}{2\beta}\arcsin\left(\frac{\beta y}{\sigma}\right) \pm \int_0^z N\, dz = \text{const} \qquad (5)$$

These curves are plotted for different values of σ and N^2 in Figure 3. When the stratification is constant, the characteristics are essentially straight lines except in the vicinity of the inertial latitudes, where the cusps imply reflections. An increase in the stratification is seen to result in characteristics that are more horizontal; this happens in the thermocline. In the deep ocean, however, the characteristics are practically

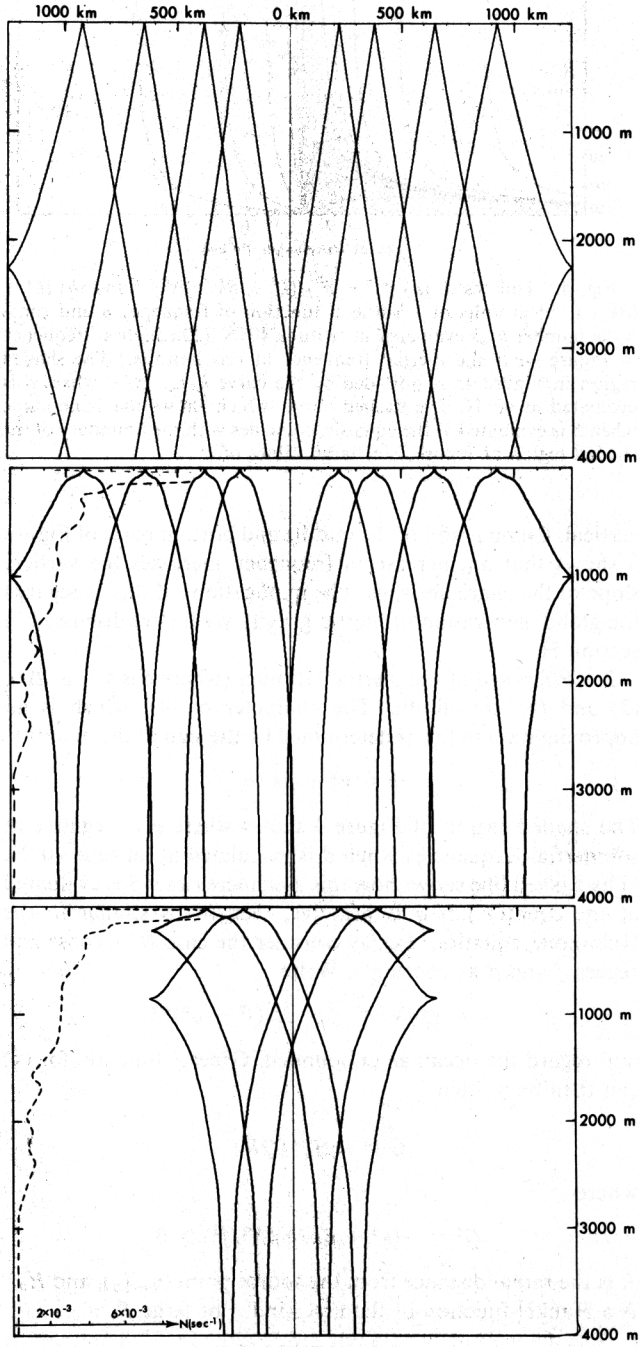

Fig. 3. (Top) Characteristics of (5) for $\sigma = 2\pi/(2.5$ days) and $N = \text{const} = 2 \times 10^{-3}$ s^{-1}. (Middle) Characteristics for $\sigma = 2\pi/(2.5$ days) and N as observed in the equatorial Atlantic. The dashed line is a plot of N, which has a maximum value of 2×10^{-2} s^{-1} at a depth of 87 m. (Bottom) Characteristics for $\sigma = 2\pi/(5$ days) and N as observed. The central vertical line is the equator.

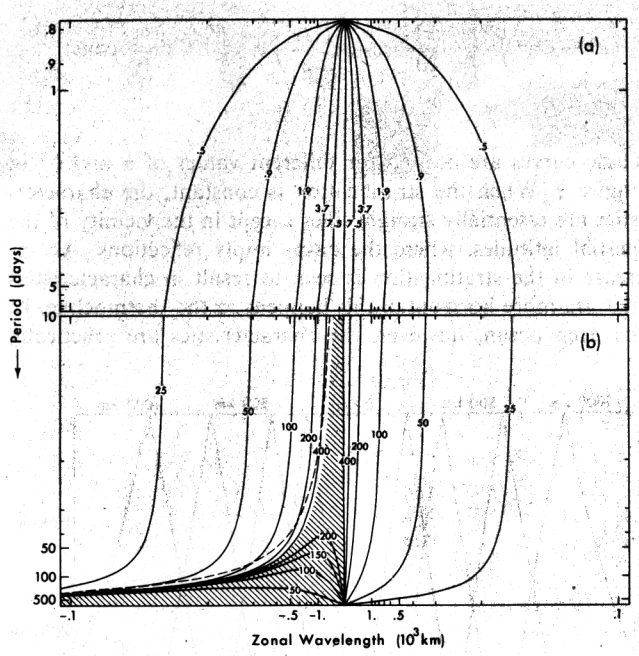

Fig. 4. Isolines of (*a*) $[(f^2 - \sigma^2)/(k^2 + \beta k/\sigma)N^2]^{1/2}$ and (*b*) $[k^2 + (\beta k/\sigma)]^{-1/2}$ in units of 1 km as a function of frequency σ and zonal wave number k as evaluated at latitude 40°N. (The highest frequency in Figure 4*a* is the inertial frequency at this latitude.) The shaded region in Figure 4*b* is bounded by the curve $k = -\beta/\sigma$, where β is evaluated at 40°N. The dashed curve, which shows the same curve when β is evaluated at the equator, coincides with the boundary of the shaded region of Figure 2 for large values of s.

vertical. Comparison of the middle and bottom parts of Figure 3 shows that an increase in frequency increases the vertical slope of the characteristics. The implications of this as regards the global generation of inertia-gravity waves are discussed in section H.

2. Poleward of the inertial latitudes (where $\cos\theta = \sigma/2\Omega$), (3) and (4) are elliptic. The character of (4), which is an approximation to (3), is determined by the sign of the quantity

$$q = k^2 + \beta k/\sigma$$

The shaded region of Figure 4 shows where q is negative at subinertial frequencies when β is calculated at latitude 40°N. (The dashed line shows how this area increases if β is evaluated at the equator.) If q is negative, then (4) is similar to the Helmholtz equation. Let us consider the case N = const and regard f and β as constants. Write

$$\eta = yf/N \qquad \zeta = zf/(f^2 - \sigma^2)^{1/2}$$

and regard the ocean as unbounded. Green's function for (4) can then be written

$$G = i\pi H_0^{(1)}(QR)$$

where

$$Q^2 = -(k^2 + \beta k/\sigma)(N^2/f^2) > 0$$

R is the radial distance from the source point (η_0, ζ_0), and $H_0^{(1)}$ is a Hankel function of the first kind. For large R,

$$G \sim (2\pi/QR)^{1/2} e^{i(QR + \pi/4)}$$

This implies that a point source in the interior of the ocean will radiate cylindrical waves. We anticipate that these are Rossby waves. The manner in which these waves radiate is to be contrasted with the propagation of inertia-gravity waves along characteristics. This Green function is valid if f and β are treated as constants. In the case of variable f, Rossby waves, like inertia-gravity waves, have turning latitudes beyond which they cannot radiate.)

3. Poleward of the inertial latitudes the response of the ocean to a forcing that has frequency σ and zonal wave number k such that

$$\bar{Q}^2 = [k^2 + (k/\sigma)\beta](N^2/f^2) > 0$$

is trapped, both vertically and horizontally, around the forcing region. This is evident from the Green function

$$G = \frac{1}{2\pi} K_0(\bar{Q}R) \sim \frac{1}{2\pi}\left(\frac{\pi}{2\bar{Q}R}\right)^{1/2} e^{-\bar{Q}R} \qquad \text{for large } R \qquad (6)$$

(This Green function is valid if f, β, and N are regarded as constants and if the ocean is assumed to be unbounded.) Isolines of the horizontal e folding distance $f/N\bar{Q}$ as a function of σ and k are shown in the unshaded part of Figure 4*b*. The continuation of these contours to higher frequencies (i.e., the domain of Figure 4*a*) is simply straight vertical lines. Isolines of the vertical e folding distance $(f^2 - \sigma^2)^{1/2}/N\bar{Q}$ as a function of k and σ are shown in Figure 4*a*. The contours in Figure 4*b* are a continuation of those in Figure 4*a* (but not vice versa) provided the numerical values are multiplied by f/N. The results are of course invalid should the e folding depth exceed the depth of the ocean. From Figure 4 we infer that the response of the ocean to forcing at frequencies slightly less than the inertial frequency is strongly trapped in the vertical. Hence energy levels in the deep ocean, but not in the surface layers, will drop sharply as the frequency decreases from slightly above to slightly below the inertial frequency. As the frequency decreases further, the forcing penetrates to greater depths—soon right to the ocean floor—so that energy levels at depth increase. Eastward propagating disturbances with very low frequencies ($\sigma \to 0$) are again strongly trapped in the vertical. The same is true of the oceanic response to atmospheric storms with small horizontal dimensions. (Some of these results were obtained by *Veronis and Stommel* [1956].) The method by which these results were obtained here is of limited validity. (The parameters f, β, and N have all been regarded as constants.) In the subsequent sections of this paper these constraints will be relaxed. By separating variables we shall obtain two representations for the solution. Each representation has advantages and disadvantages, but they fortunately complement each other.

b. Separation of variables. Write

$$\begin{bmatrix} u\sin\theta \\ iv\sin\theta \\ P \end{bmatrix} = 2\Omega a Z(z) e^{i(s\phi - \sigma t)} \begin{bmatrix} U(\theta) \\ V(\theta) \\ 2\Omega\rho_0 a P(\theta) \end{bmatrix} \qquad (7a)$$

$$\begin{bmatrix} w \\ \rho \end{bmatrix} = 2\Omega a W(z) e^{i(s\phi - \sigma t)} \begin{bmatrix} iP(\theta) \\ [\bar{\rho}_z P(\theta)]/\sigma \end{bmatrix} \qquad (7b)$$

and assume for the moment that equations (1) are homogeneous; then the vertical structure of the solution is described by

$$W_{zz} + \frac{N^2\epsilon}{4\Omega^2 a^2} W = 0 \qquad (8a)$$

or

$$\frac{\partial}{\partial z}\left(\frac{1}{N^2}\frac{\partial Z}{\partial z}\right) + \frac{\epsilon}{4\Omega^2 a^2} Z = 0 \qquad (8b)$$

where

$$W = \frac{2\Omega\sigma a}{N^2}\frac{\partial Z}{\partial z}$$

The boundary conditions are

$$W = 0 \quad \text{or} \quad Z_z = 0 \qquad z = -H \tag{9a}$$

$$W_z - \frac{\epsilon g}{4\Omega^2 a^2}W = 0 \quad \text{or} \quad Z_z + \frac{N^2}{g}Z = 0 \qquad z = 0 \tag{9b}$$

The latitudinal structure is described by Laplace's tidal equation (LTE)

$$L(P) - \epsilon P = 0 \tag{10}$$

or by an equivalent equation for the meridional velocity component (see Appendix B). On a β plane this equation is

$$V_{yy} + \left(\frac{\sigma^2}{gh} - k^2 - \frac{\beta k}{\sigma} - \frac{f^2}{gh}\right)V = 0 \tag{11}$$

There are (at least) two ways in which equations (1) can be solved. One way is to solve equation (8) first; thus one obtains a complete set of eigenfunctions W_n (or Z_n) and eigenvalues ϵ_n. If the forcing function is a body force (and not an imposed surface pressure, for example) and if its vertical and latitudinal dependencies are separable, then its vertical structure can be expanded in a series of these vertical modes. It then remains to solve (10) for given values of ϵ ($= \epsilon_n$) and with the appropriate component of the forcing function on the right-hand side of the equation. If we rewrite the eigenvalues ϵ_n of the Sturm-Liouville problem (equations (8) and (9)) as

$$\epsilon_n = 4\Omega^2 a^2/gh_n$$

then the homogeneous equation (10) is Laplace's tidal equation with the actual depth H of the ocean replaced by an equivalent depth h_n. The vertical structure equation thus determines the equivalent depths associated with the baroclinic modes. (We shall find that all the h_n are positive.) The solution to the inhomogeneous version of (10) can be expressed in terms of the eigenfunctions of the homogeneous equation (10). The eigenvalue of this equation is the frequency λ. The eigenfunctions are referred to as Hough functions in honour of *Hough* [1898], who solved Laplace's tidal equations for small values of ϵ_n (large values of h_n).

Equations (1) can alternatively be solved by first determining the eigenfunctions of LTE, with the constant of separation ϵ, however, regarded as the eigenvalue. The forcing function can then be projected onto these latitudinal modes, and it remains to solve an inhomogeneous version of the vertical structure equation (equation (8)) for various given values of ϵ. It is clear from (8) that for positive values of ϵ the solution can be interpreted as propagating waves, but for negative values of ϵ the response is vertically trapped near the forcing region. The parameter $\epsilon^{-1/2}$ is a measure of the vertical wavelength.

The first method, in which the solution is expressed in terms of standing vertical modes, is commonly used in studies of the response of the ocean to atmospheric forcing. The appeal of this method is its simplicity: given the mean Väisälä frequency of the oceans (as a function of depth), it is immediately possible to calculate the vertical modes without having to specify the forcing function (provided it can be regarded as a body force in a mixed surface layer). The representation of the solution obtained in this manner readily provides information about the horizontal structure of the response of the ocean to atmospheric forcing. However, since practical considerations dictate that all but the barotropic and first few baroclinic modes be disregarded, it is difficult to obtain information about motion that is vertically trapped near the forcing region or that is vertically propagating. The measurements of *Sanford* [1975] and *Weisberg et al.* [1977] give evidence of vertically propagating waves in mid-latitude and equatorial regions, respectively. *Tyabin and Sleptsov-Shevlevich*'s [1975] analysis of the response of the ocean to atmospheric storms coming off Africa indicates that this response is vertically trapped near the forcing region. These measurements suggest that under certain conditions it is impossible to describe the oceanic response in terms of one or two standing vertical modes.

Atmospheric tides [*Chapman and Lindzen,* 1970] and forced atmospheric waves of lower frequencies [*Holton,* 1975] are studied by projecting the forcing function onto vertically propagating latitudinal modes. These modes are eigenfunctions of LTE when ϵ is the eigenvalue. The modes and associated eigenvalues are confusingly referred to as Hough functions and equivalent depths, respectively. (This set of eigenfunctions is very different from the set that is obtained from LTE when the frequency is the eigenvalue.) The complete set of eigenfunctions and eigenvalues includes both positive and negative 'equivalent depths' [*Dikii,* 1965]. This is to be contrasted with the eigenvalue problem posed by (8) and (9), which yield positive equivalent depths only. The physical significance of the term negative equivalent depth is not immediately clear—it suggests that the ocean is unstably stratified [*Longuet-Higgins,* 1968]—unless it is kept in mind that h_t is effectively the square of a vertical wavelength. As was pointed out earlier, positive equivalent depths are associated with vertically propagating waves, and negative equivalent depths with vertically trapped waves. *Lindzen* [1966] and *Kato* [1966] first pointed out the role that these negative eigenvalues play in the problem of forced waves.

The second (meteorological) method of solution appears cumbersome in comparison with the first method, which involves the vertical baroclinic modes: it is necessary to know the frequency σ and zonal wave number k of the forcing at the outset, because there is a different set of eigenfunctions: equivalent depths for each (σ, k) combination. Furthermore, the response of the ocean cannot be studied locally (even if the response is local) because the eigenfunctions cover the sphere. This method is nonetheless of great value because it gives detailed information about the vertical structure of oceanic motion, and it enables identification of the factors that can prevent the establishment of vertical baroclinic modes.

C. The Forcing Function

In equations (1) the surface wind stress is treated as a body force in a mixed surface layer of depth D. Atmospheric pressure disturbances that can generate oceanic motion appear in the boundary condition in (2*b*). It is therefore not immediately possible to compare the relative importance of these two types of forcing. Since the pressure in the mixed surface layer of depth D is

$$P = PA + g\rho_0\eta$$

where η is the elevation of free surface, and since

$$\eta_t = w_s$$

where w_s is the vertical velocity at the free surface, it is possible to derive the following equation for the vertical velocity in the

mixed surface layer (where $N^2 = 0$):

$$\bar{L}(w) = \hat{k}\cdot\text{curl}\left(\frac{f\tau}{\sigma^2 - f^2}\right) + i\sigma\,\text{div}\left(\frac{\tau}{\sigma^2 - f^2}\right)$$

$$- i\sigma D\nabla^2\frac{PA}{\sigma^2 - f^2} + \frac{D}{a}\frac{\partial}{\partial\theta}\frac{f}{\sigma^2 - f^2}\frac{1}{a\sin\theta}\frac{\partial PA}{\partial\phi} \qquad (12)$$

The complicated operator $\bar{L}$ need not concern us; this equation is of interest only because it permits us to compare the relative importance of wind stress and pressure forcing. If we make the β plane approximations (see Appendix B), then (12) yields

forcing function =

$$-f\hat{k}\cdot\text{curl}\,\tau - \beta\tau^x - \frac{\partial}{\partial t}\,\text{div}\,\tau + D\beta PA_x + D\nabla^2 PA_t \qquad (13)$$

A B C D E

plus terms proportional to βf. The vector operators now appear in their Cartesian form. Let $|PA|$ and $|\tau|$ denote the characteristic amplitudes of the pressure fluctuations and wind stress, and let L and T be the characteristic length and time scales of the forcing. The relative importance of each of the terms in (13) is then

$$\frac{f|\tau|}{L} \quad \beta|\tau^x| \quad \frac{|\tau|}{LT} \quad \frac{D\beta|PA|}{L} \quad \frac{D|PA|}{L^2T} \qquad (14)$$

A B C D E

Observe that the ratio of term C to term B is the same as the ratio of term D to term E. Hence a rearrangement of the terms in (14) is

$$T f|\tau| \quad (1 + \beta LT)|\tau| \quad (1 + \beta LT)\frac{D|PA|}{L} \qquad (15)$$

A C + B E + D

Take $D = 50$ m, $|\tau| = 1$ dyn/cm², and $|PA| = 4$ mbar $= 10^3$ dyn/cm². (In severe storms, $|PA|$ can be as large as 50 mbar.) Figure 5 shows the importance of the various terms as a function of L and T. For storms with a period of 1 day and a scale of 200–400 km, all the terms are nearly equally important (if we are in the vicinity of 30°N or 30°S). The importance of term A decreases with a decrease in latitude. Regions of the L-T diagram where the different terms dominate are indicated in the figure by the appropriate letters. Pressure fluctuations are most important when the length scale L is small. The divergence of the wind stress is most significant when the time scale is short.

The manner in which the ocean responds to this forcing is the subject of the following sections. We shall find that inertia-gravity waves are excited by (relatively) high-frequency disturbances so that terms A, C, and E are most important. I. Orlanski (unpublished manuscript, 1970) has pointed out that because pressure fluctuations, unlike the wind stress, do not act through a mixed layer which takes a certain time to become established, they are particularly effective for the generation of inertia-gravity waves. Rossby waves are generated by westward propagating disturbances with low periods so that terms A, B, and D matter most. (The area under the hyperbola $\beta LT = 2$ corresponds to the shaded part of Figure 4.) We shall find

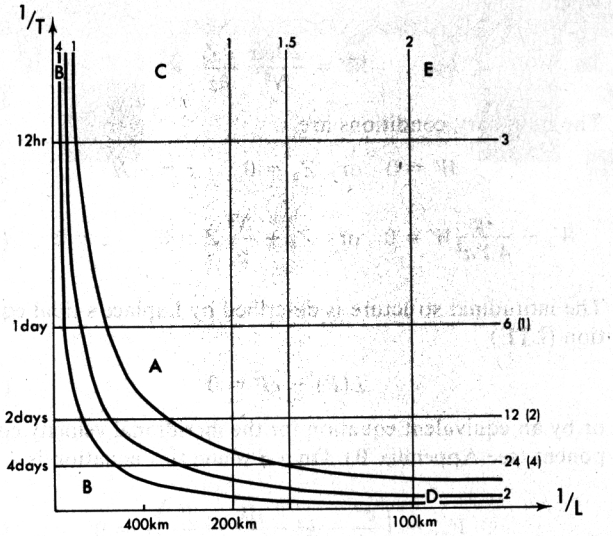

Fig. 5. Relative importance of the various terms in (15) as a function of the time scale T and the length scale L of the forcing function. Vertical lines are $(D|PA|/L) = \text{const}$. Horizontal lines are $Tf = \text{const}$. Hyperbolae are $\beta LT = \text{const}$. The values of the constants are given on the lines. In the case of horizontal lines the constants are for f at 30°N and 9°N. Parameter β is evaluated at 30°N. The letters A, B, etc. indicate the regions where the different terms in (15) are dominant.

that there are wide bands of frequencies and wave numbers for which no oceanic waves are excited; the response is simply trapped in the vicinity of the forcing region.

D. Vertically Propagating Latitudinal Modes

This section concerns a description of the oceanic response, to forcing at a given frequency and zonal wave number, in terms of vertically propagating and vertically trapped latitudinal modes. These modes are eigenfunctions of Laplace's tidal equations, and each mode is associated with an equivalent depth h_l (or ϵ_l). In order to have an appreciation for the significance of the different values that h_l can assume, we start by describing the solution to the vertical structure equation for a wide range of values of h_l.

1. *Vertical Structure*

The equation that describes the vertical structure is

$$W_{zz} + (N^2/gh)W = F_l \qquad (16)$$

where F_l is the projection of the forcing function onto the latitudinal mode under consideration. We regard F_n as a constant in a surface layer of depth 50 m. Below that, its value is zero.

Equation (16) is to be compared with the equation that describes the vertical propagation of internal gravity waves in a stratified nonrotating fluid:

$$W_{zz} + [(N^2/\sigma^2) - 1]k^2W = 0 \qquad (17)$$

(See, for example, *Turner* [1973].) If $\sigma \ll N$, then we recover (16), which therefore is merely the equation for low-frequency internal gravity waves. The effects of rotation and the variable Coriolis parameter enter through the parameter h_l. For a given value of h_l the solutions of (16) are either oscillatory everywhere or exponential everywhere. Equation (17), on the other hand, can for a given frequency have solutions that are oscillatory in some regions (where $\sigma < N$) and exponentially decaying in others (where $\sigma > N$). Hence trapped oscillatory modes

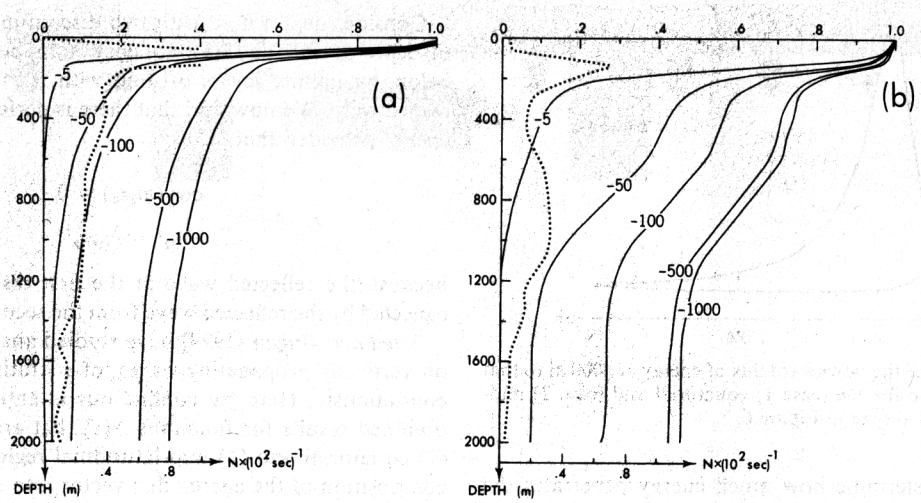

Fig. 6. The oceanic response for various negative values of the equivalent depth for thermoclines representative tropical oceans and (*b*) mid-latitude oceans. The dotted lines show $N(z)$, which in Figure 6*a* has a maximum value of 2×10^{-2} s^{-1} at 87 m. The function plotted is $Z(z)$ of (7*a*), normalized with respect to its value at the surface.

in the thermocline (where N has a maximum) are possible. By confining attention to hydrostatic motion, for which $\sigma \ll N$, we are precluding such possibilities.

a. Negative equivalent depths. If $h_l < 0$, then (16) has exponentially decaying solutions so that the response of the ocean is vertically trapped near the forcing region. For constant values N the vertical e folding depth is $(g|h|)^{1/2}/N$. The smaller $|h_l|$ and the larger N, the more severe the trapping. Figure 6 shows the amplitude of the response, as a function of depth, for different negative values of h, for different values of N: Figure 6*a* is representative of the tropical oceans; Figure 6*b*, which has a deep thermocline, is representative of the North Atlantic. (The minimum that N has at a depth of about 400 m is apparently the result of communication with the Polar Sea.) Figure 6 shows that the sharp thermocline in the tropics prevents the effect of the forcing from penetrating to great depths (unless h is very large and negative). The deep thermocline, between 600 and 1200 m in Figure 6*b*, similarly attenuates the oceanic response.

The results of Figure 6 are for body forces (due to the wind stress) in a mixed surface layer 50 m deep. If instead the forcing is due to atmospheric pressure fluctuations, which affect the surface boundary conditions (see equation (2*b*)), then a mixed surface layer need not be involved, but the oceanic response for $h_l < 0$ will be essentially the same. Hence for small negative h_l, the amplitude of the vertical displacement of fluid particles (in response to the forcing) decays exponentially downward into the interior of the ocean. In such cases the ocean is said to behave as an 'inverted barometer.' We shall know for which frequency–wave number ranges to expect such a behavior if we know the ranges for which h_l is small and negative.

b. Positive equivalent depths. For positive values of h_l, (16) has solutions that represent vertically propagating waves. If

$$m = N(z)/(gh_l)^{1/2} \tag{17'}$$

is large, then the WKBJ approximation gives

$$W \sim \frac{1}{[m(z)]^{1/2}} \exp\left[\pm i \int m(z)\, dz\right] \tag{17''}$$

Hence m, as given by (17'), is the 'local' wave number, which increases as N increases. If the waves become very short, they are associated with large vertical shears and are likely to break or are prone to dissipation. Short waves are therefore unlikely to penetrate very sharp thermoclines, such as the ones in the tropics.

The above remarks are valid when the vertical scale of the waves is short in comparison with the scale of vertical variation of $N(z)$. Consider next the opposite extreme, namely, a wave incident on a discontinuity of $N(z)$, where the value of N abruptly changes from a constant N_1 to a different constant N_2. The waves transmitted across this discontinuity have amplitude

$$T = 2I/(1 + N_2/N_1) \tag{18a}$$

The reflected wave has amplitude

$$R = \frac{N_1 - N_2}{N_1 + N_2} I \tag{18b}$$

where I is the amplitude of the incident wave. The parameter T is independent of wavelength. As the ratio N_2/N_1 increases, the amplitude of the vertical velocity below the discontinuity becomes smaller. If, however, $N_2 > N_1$, then the amplitude of the vertical velocity below the discontinuity is greater than that above the thermocline. This is consistent with the results of (17), but it does show that T is not a measure of the energy that penetrates the thermocline.

Consider the quantity

$$J = W^* W_z - W W_z^* \tag{19}$$

where W^* is the complex conjugate of W. It follows from the homogeneous equation (16) that J, which is a purely imaginary number, is independent of depth. Since the pressure is proportional to W_z, J is essentially the vertical energy flux [see *Eliassen and Palm*, 1960]. If the vertical velocity is of the form e^{imz}, then

$$J \sim |mW^2|$$

This quantity is a constant for the expression in (17), which implies that the vertical flux of energy is a constant for very short waves. In general, variations in N can reflect certain

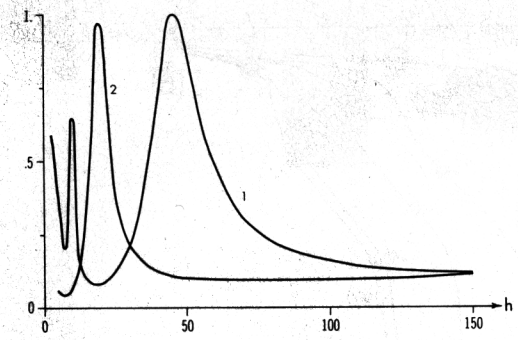

Fig. 7. The ratio of the downward flux of energy at 4000 m to that above the thermocline for the (case 1) equatorial and (case 2) mid-latitude stratifications shown in Figure 6.

wavelengths. To determine how much energy penetrates the thermocline, for example, it is necessary to calculate the ratio $\bar{J} = J_1/J_0$, where J_1 and J_0 are the contributions to J due to downward propagating waves below and above the thermocline, respectively. For the step discontinuity in stratification just described,

$$|\bar{J}| = 4N_1N_2/(N_1 + N_2)^2 \tag{20}$$

the maximum transmission of energy occurs when $N_2 = N_1$. For large or small values of N_2/N_1, little energy propagates across the discontinuity. A downward propagating internal gravity wave reflects completely when it encounters a layer of very large stability ($N_2 \to \infty$) or a homogeneous layer ($N_2 = 0$). (Although the latter result is correct, it cannot be inferred from this analysis, in which it is assumed that $\sigma < N_2$.)

Consider next a fluid with two discontinuities in N: a layer of depth z_0 and Väisälä frequency N_2 is bounded above and below by infinite layers of fluid with $N = N_1$ and $N = N_3$, respectively. We now find that there is perfect transmission of energy provided that

$$\cos(m_2 z_0) = 0 \tag{21}$$

$$m_2^2 = m_1 m_3 \tag{22}$$

because the reflected wave at the first discontinuity in N is canceled by the reflected wave from the second discontinuity.

Mied and Dugan [1974] have studied analytically the effect, on vertically propagating waves, of a stratification that varies continuously. Here we confine our attention to numerically obtained results for functions $N(z)$ that are representative of (1) equatorial and (2) mid-latitudinal regions. To permit decomposition of the energy flux vector into upward and downward components, it is assumed that there are regions where N has constant values above the thermocline and below 4000 m. A radiation condition—downward flux of energy only—is imposed below 4000 m. The results are shown in Figure 7, from which it is evident that for certain values of h (45, 10, and 3 cm for case 1 and 25 and 3 cm for case 2) the ocean is transparent, and energy readily propagates from the surface to the ocean floor. These values of h are effectively the solutions to (21). Long vertical waves ($50 < h < 500$ cm), however, undergo considerable internal reflection, and less than 20% of their energy penetrates to the ocean floor.

The discussion thus far has concerned solutions to the homogeneous version of (16) with a radiation condition imposed at depth. Solutions to the nonhomogeneous equation (16),

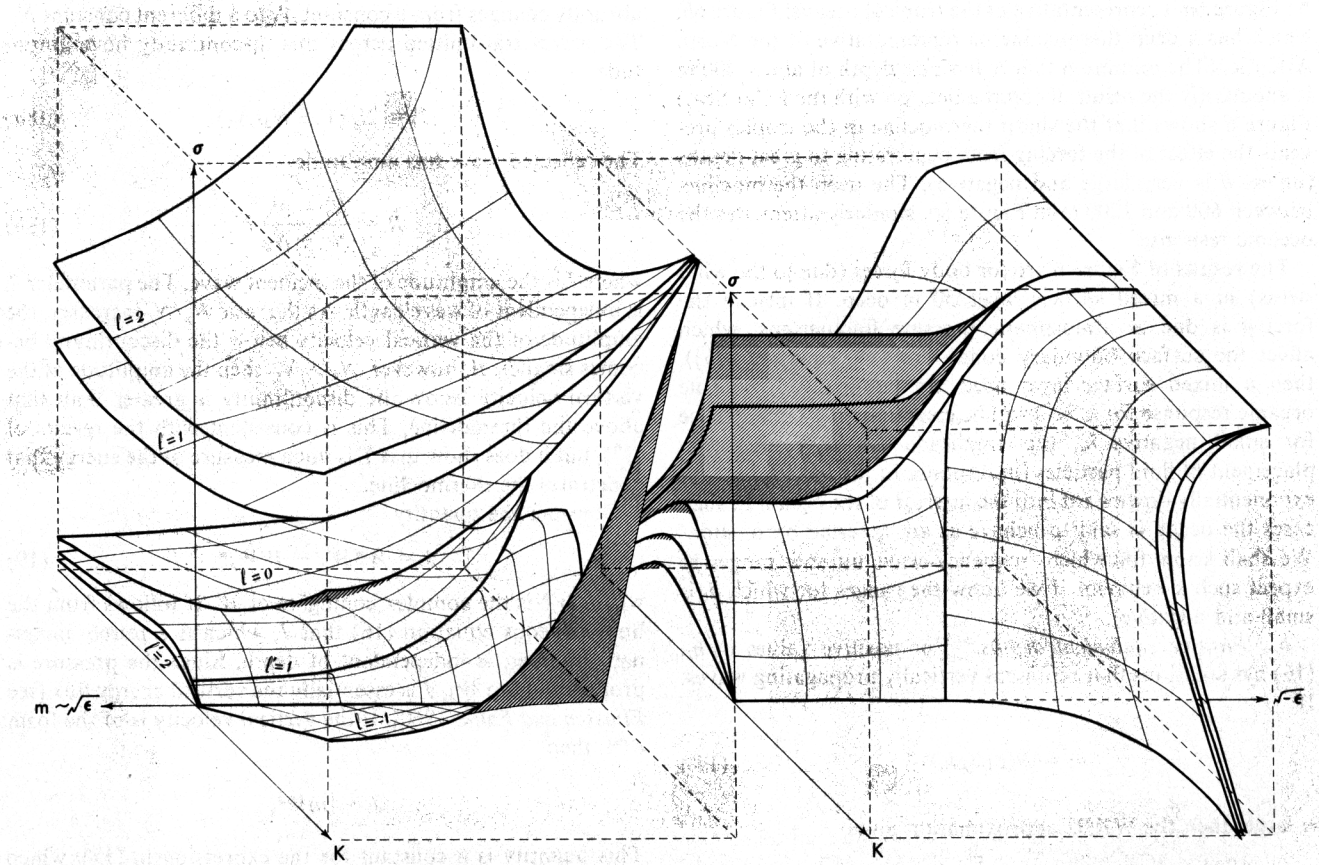

Fig. 8. Schematic dispersion diagram for free and forced waves on a sphere. (This is a modified version of a figure in the thesis by *Moura* [1975].) Figures 9, 16, and 20 are effectively sections from this figure.

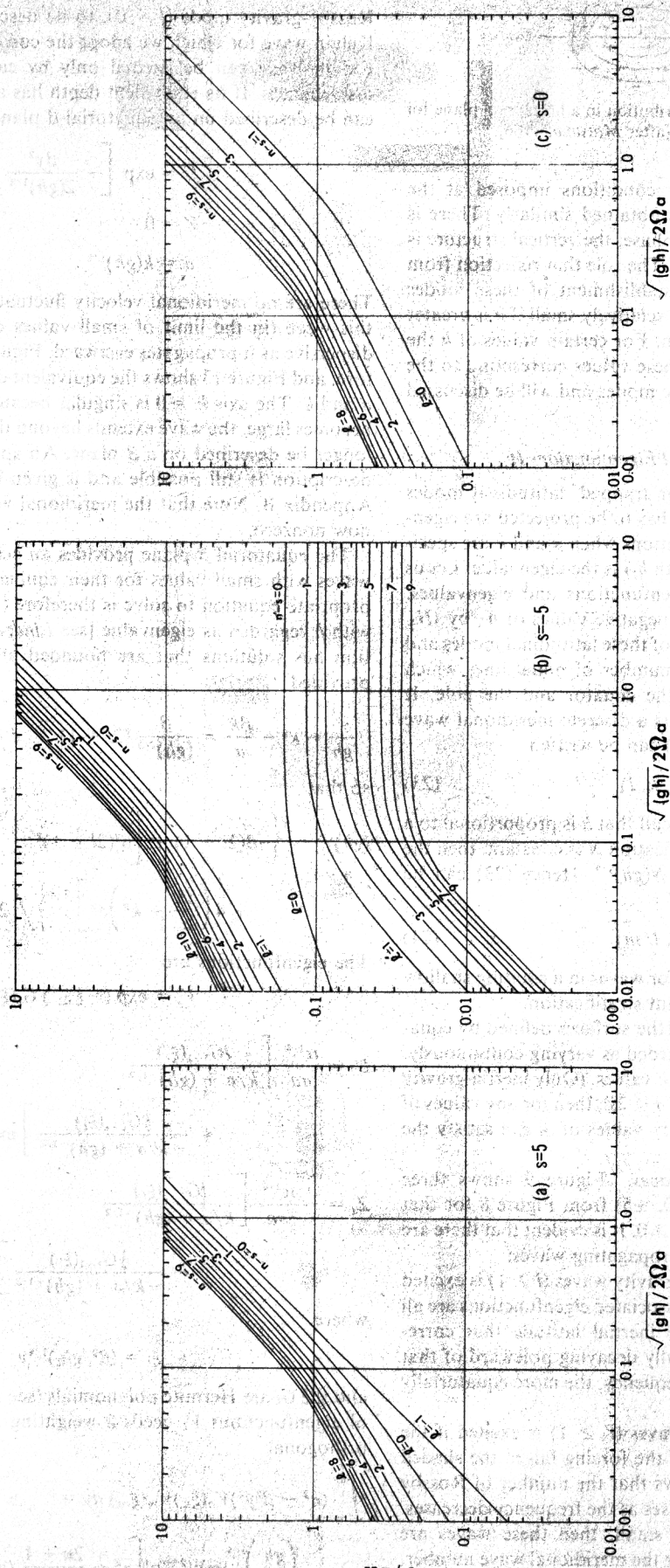

Fig. 9. Three sections from Figure 8 along $s = 0, \pm 5$ that show the equivalent depth as a function of frequency [after *Longuet-Higgins*, 1968].

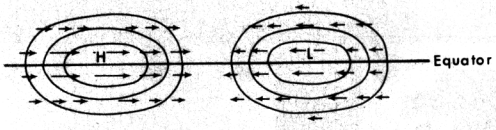

Fig. 10. Velocity and pressure distribution in a horizontal plane for equatorial Kelvin waves [after *Matsuno*, 1966].

with the appropriate boundary conditions imposed at the ocean floor and surface, can be obtained similarly. There is now no vertical propagation of phase; the vertical structure is similar to that of a forced mode. The role that reflection from the ocean floor plays in the establishment of these modes depends on the value of h and is relatively small if h is greater than 50 cm but less than 500 cm. For certain values of h the oceanic response is resonant. These values correspond to the natural baroclinic and barotropic modes and will be discussed further in section E.

2. *Eigenvalues h_l and Latitudinal Eigenfunctions H_l*

The vertically propagating, or trapped, latitudinal modes onto which the forcing function has to be projected are eigenfunctions of Laplace's tidal equations when σ and k are specified and ϵ (or the equivalent depth h_l) is the eigenvalue. Let us denote the complete set of eigenfunctions and eigenvalues, which will include positive and negative values of h_l, by $\{H_l, h_l\}$. The index l is the 'signature' of these latitudinal modes and will be found to represent the number of nodal lines which these functions have between the equator and the pole. It follows that l can be regarded as a discrete meridional wave number. The eigenvalues of (10) can be written

$$h = h(\sigma, k, l) \tag{23}$$

From the previous section we recall that h is proportional to a vertical wavelength. If the stratification N is constant, then the vertical wave number is $m = N(gh)^{1/2}$. Hence (23) can be rewritten

$$\sigma = \sigma(k, l, m) \tag{24}$$

which is the dispersion relation for waves in a rotating shallow spherical shell of fluid of constant stratification.

Figure 8 schematically shows the surfaces defined by equation (24) when m and k are regarded as varying continuously. For $\sigma < 2\Omega$, m is real for any σ, k values. (Only inertia-gravity waves are excited in this case.) If $\sigma < 2\Omega$, then for any values of σ and k, both real and imaginary values of m can satisfy the dispersion relation.

a. Vertically propagating waves. Figure 9 shows three sections (along the planes $s = 0, \pm 5$) from Figure 8 for that range of parameters for which $h > 0$. It is evident that there are two principal classes of freely propagating waves:

1. An infinite set of inertia-gravity waves ($l \geq 1$) is excited for any values of σ and k. The associated eigenfunctions are all sinusoidal equatorward of the inertial latitude that corresponds to σ and are exponentially decaying poleward of that latitude. Hence the lower the frequency, the more equatorially trapped the waves.

2. A finite set of Rossby waves ($l' \geq 1$) is excited if the frequency and wave number of the forcing fall in the shaded part of Figure 2. Figure 9 shows that the number of Rossby waves that can be excited increases as the frequency decreases. If their equivalent depths are small, then these waves are equatorially trapped. The higher the meridional wave number, the further poleward the Rossby waves extend.

There are two additional waves that can be excited: a Rossby-gravity mode ($l = 0$), to be described shortly, and a Kelvin wave for which we adopt the convention $l' = -1$. The Kelvin wave can be excited only by eastward propagating disturbances. If its equivalent depth has a small value, then it can be described on an equatorial β plane (see Appendix B):

$$U = \exp\left[-\frac{\beta y^2}{2(gh)^{1/2}}\right] \tag{25a}$$

$$V = 0 \tag{25b}$$

$$\sigma = k(gh)^{1/2} \tag{26}$$

There are no meridional velocity fluctuations associated with this wave (in the limit of small values of h), and it is nondispersive as it propagates eastward. Figure 10 shows its structure, and Figure 13 shows the equivalent depth as a function of σ and k. The axis $k = 0$ is singular because $h \to \infty$ there. As h becomes large, the wave extends beyond the tropics and can no longer be described on a β plane. An approximate analytical description is still possible and is given by equations (B5) in Appendix B. Note that the meridional velocity component is now nonzero.

The equatorial β plane provides an accurate description of waves with small values for their equivalent depths. The appropriate equation to solve is therefore (11), with $f = \beta y$ and with h regarded as eigenvalue [see *Lindzen*, 1967]. This equation has solutions that are bounded at large values of $|y|$ provided

$$\frac{\sigma^2}{gh} - k^2 - \frac{\beta k}{\sigma} = \frac{\beta}{(gh)^{1/2}}(2l + 1) \qquad l = 0, 1, 2, \cdots \tag{27}$$

so that

$$(gh)^{1/2} = \left\{-\beta(2l + 1) \pm \left[\beta^2(2l + 1)^2 + 4\left(\frac{\beta k}{\sigma} + k^2\right)\sigma^2\right]^{1/2}\right\} \Big/ 2\left(k^2 + \frac{\beta k}{\sigma}\right) \tag{28}$$

The eigenfunctions are

$$V_l = \exp(-\tfrac{1}{2}\xi_l^2)\, G_l(\xi_l) \tag{29a}$$

$$U_l = \frac{i\epsilon^{1/4}}{\sigma a}\left[\frac{lG_{l-1}(\xi_l)}{k/\sigma + (gh)^{-1/2}} + \frac{\tfrac{1}{2}G_{l+1}(\xi_l)}{-k/\sigma + (gh)^{-1/2}}\right]\exp(-\tfrac{1}{2}\xi_l^2) \tag{29b}$$

$$Z_l = -\frac{i\epsilon^{1/4}}{\sigma a}\left[\frac{lG_{l-1}(\xi_l)}{k/\sigma + (gh)^{-1/2}} - \frac{\tfrac{1}{2}G_{l+1}(\xi_l)}{-k/\sigma + (gh)^{-1/2}}\right]\exp(-\tfrac{1}{2}\xi_l^2) \tag{29c}$$

where

$$\xi_l = (\beta^2/gh_l)^{1/4} y$$

and the G_l are Hermite polynomials (see Appendix A). The set of eigenfunctions V_l needs a weighting factor in order to be orthogonal:

$$\int_{-\infty}^{\infty} (\sigma^2 - \beta^2 y^2) V_n(\xi_n) V_m(\xi_m)\, dy = \left(\frac{gh}{\beta^2}\right)^{1/4} (\pi)^{1/2} 2^n n! \left[\sigma^2 - \frac{2n + 1}{2}(gh\beta^2)^{1/2}\right]\delta_{mn} \tag{30}$$

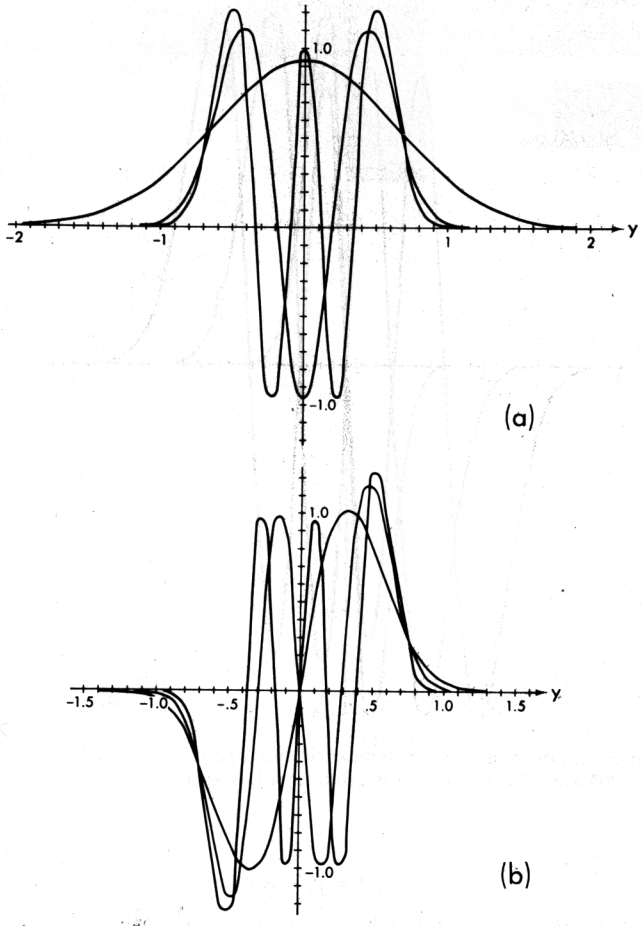

Fig. 11. Latitudinal structure of the meridional velocity component of the gravest (*a*) symmetric and (*b*) antisymmetric westward propagating, inertia-gravity waves with a period of 5 days and a wavelength of 2000 km. Distance from the equator is given in units of 1000 km.

where $\delta_{mn} = 0$ if $m \neq n$ and $\delta_{mn} = 1$ if $m = n$. Care must be taken in the evaluation of this integral, since the y domain on a sphere is finite. We shall find that (30) can be used for the normalization of low-frequency inertia-gravity waves of any meridional (l) order; in the case of Rossby waves it can only be used if $l \sim O(1)$.

The gravest antisymmetric mode ($l = 0$) deserves special attention. For this Rossby-gravity wave,

$$(gh)^{1/2} = \sigma^2/(\beta + \sigma k) \quad \text{or} \quad -\sigma/k \tag{31}$$

The second root has to be discarded because the associated zonal velocity field (equation (29*b*)) is singular even though the meridional velocity field is bounded.

For $l \geq 1$, (28) yields two roots: h_l^+ and h_l^-. For large values of l,

$$(gh_l^+)^{1/2} \to \sigma^2/\beta(2l + 1) \tag{32}$$

It follows that the turning latitude y_T for solutions of (11),

$$y_T^2 = (2l + 1)(gh)^{1/2}/\beta \to \sigma^2/\beta^2 \tag{33}$$

in the limit in (32). This is simply the inertial latitude. The h_l^+ solutions to (29) therefore yield the equivalent depths for the inertia-gravity waves. Figure 11 shows the first few modes for a choice of σ and k that corresponds to equatorially trapped waves which have been observed (see section H). Note how rapidly the turning latitude approaches the inertial latitude as l increases.

It follows from (32) that the integral in (30) is always positive for the h_l^+. It can therefore be used for normalization purposes.

The h_l^- solutions to (28) are associated with Rossby waves. For large values of l,

$$(gh_l^-)^{1/2} \to -\frac{\beta}{k^2 + \frac{\beta k}{\sigma}}(2l + 1) - \frac{\sigma^2}{\beta(2l + 1)} \tag{34}$$

Hence the turning latitude of the eigenfunctions increases as l increases. Only the gravest modes can be approximated by an equatorial β plane. *Lindzen* [1967] has suggested that only modes for which the distance y_T in (33) is less than the distance from the equator to the pole are valid. *Longuet-Higgins*'s [1968] accurate calculations for waves on a sphere show that only a finite number of Rossby modes are permissible. The equatorial β plane approximates the gravest of these modes and not, for example, those for which $h = \infty$. Figure 12 shows the gravest Rossby waves for values of σ and k that correspond to a wave in the tropical winds (see section H).

For high meridional wave numbers l the equivalent depths for inertia-gravity waves are small, but for Rossby waves the values are large. This implies that in extraequatorial regions the vertically propagating inertia-gravity waves have short vertical wavelengths but the Rossby waves should have long vertical wavelengths. Thus the vertical structure of the Rossby waves, but not of the inertia-gravity waves, will correspond to a superposition of the gravest vertical modes.

Figure 13 enables us to read off the equivalent depths for the four gravest equatorially trapped waves, for given values of σ and k. The Kelvin and Rossby-gravity waves both have group velocities to the east for all frequencies, though the phase velocity of the Rossby-gravity wave can be westward. For the higher-order Rossby and inertia-gravity waves ($l \geq 1$) the zonal group velocity vanishes when

$$k = -\beta/2\sigma \tag{35}$$

The dotted lines in Figure 13 correspond to this equation. Rossby waves with a longer (shorter) wavelength have westward (eastward) group velocities, but the phase velocity is always westward. It follows that in the absence of coasts, Rossby waves can only be excited by westward propagating disturbances, and the Kelvin wave only by eastward propagating disturbances. The equivalent depth determines the latitudinal scale of the modes (see (29*c*)), so that Figure 13 is invalid for those frequency–wave number ranges where the value of h is large. (The equatorial β plane does not adequately describe the associated eigenfunctions.) In the case of Rossby and Rossby-gravity waves, $h \to \infty$ along the curve

$$k = -\beta/\sigma \tag{36}$$

The axis $k = 0$ is another singular curve for Kelvin and Rossby waves. The appropriate dispersion relations in these limiting cases will be discussed shortly. Figure 13 shows that the Rossby-gravity wave is unlikely to be important in the response of the ocean to forcing at frequencies equal to or lower than the seasonal one. The small values of the equivalent depths at low frequencies imply very short vertical wavelengths and very small latitudinal scales. (If $h = 60$ cm, the latitudinal scale is 325 km, and if $h = 0.06$ cm, it is 60 km.) The implied vertical and horizontal shears are probably too large for the waves to be stable.

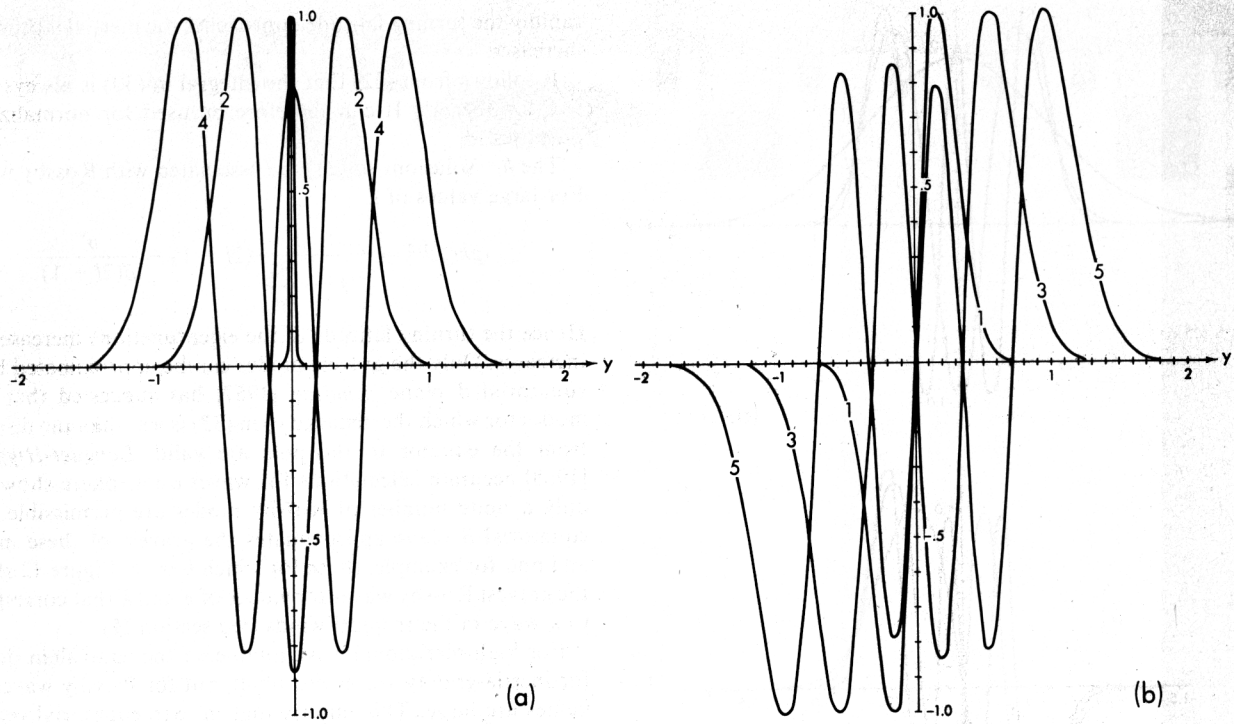

Fig. 12. Latitudinal structure of the meridional velocity component of the gravest (*a*) symmetric and (*b*) antisymmetric Rossby waves with a period of 45 days and a wavelength of 2000 km. (Normalization is arbitrary.) Distance from the equator is given in units of 1000 km.

The relative magnitudes of the vertical phase and group velocities of the four gravest equatorial modes can be inferred from Figure 14. It is evident not only that all low-frequency waves have short vertical wavelengths but also that their vertical group velocities are very small. Waves of higher frequency are therefore more likely to penetrate into the deep ocean. The zonal wavelength is another factor that affects vertical propagation. For example, eastward propagating atmospheric waves of small horizontal dimensions ($1/k$ = 100 km) excite low-frequency Kelvin waves with large vertical group velocities more readily than do waves that have large horizontal dimensions ($1/k$ = 1000 km, for example).

The frequencies of Kelvin and inertia-gravity waves appear to become infinitely large as the vertical wave number approaches zero. This is a consequence of the hydrostatic approximation. The maximum frequency for these waves is of course N. Note that the Rossby and Rossby-gravity waves have finite frequencies (considerably less than N, see Figure 2) when the vertical wave number is zero.

The description of the eigenfunctions and eigenvalues given above is inaccurate when the eigenfunctions have a significant amplitude outside the tropics. This happens when the equivalent depth becomes large ($h \to \infty$ or $\epsilon \to 0$) or when the meridional wave number l of a Rossby wave becomes large. If the mode under consideration has a turning latitude in midlatitudes, then it can be described in terms of spheroidal wave functions. If the turning latitude is close to the pole so that the mode is sinusoidal over the globe, then it can be described in terms of associated Legendre functions. In the latter limit the inertia-gravity waves are irrotational, and the Rossby waves are nondivergent. (See (B6)–(B9) in Appendix B.)

For a local description of modes that extend into midlatitudes and high latitudes, one can use the β plane equation (equation (11)). This equation is accurate, but difficult to solve, if

$$f = f_0 + \beta y$$

It is often assumed that f has a constant value f_0, in which case the latitudinal structure of the modes is described by e^{ily}. (This approximation is valid for high meridional wave numbers l but does not describe a mode in the vicinity of its turning latitude.)

The dispersion relation is

$$gh = (\sigma^2 - f_0^2)/(k^2 + l^2 + \beta k/\sigma) \qquad (37)$$

In a low-frequency limit ($\sigma \ll f_0$) that filters out inertia-gravity waves, and in a high-frequency limit that filters out Rossby waves (so that the term $\beta k/\sigma$ is negligible), the dispersion relation (37) is formally correct. (See Appendix B.)

Figure 15 is a dispersion diagram based on (37). Note that the inertia-gravity and Rossby waves are widely separated in frequency and that the Rossby-gravity and Kelvin waves are absent because they are grave modes ($l \sim O(1)$). The inertia-gravity waves have a cutoff frequency at the inertial frequency. Waves with a period exactly equal to the inertial period have zero vertical wavelength and zero vertical group velocity. Such waves, which are predominantly excited by atmospheric forcing of large horizontal extent (small k and l), should therefore be expected in the surface layers of the ocean only. Small atmospheric storms will excite waves that propagate vertically quite rapidly and that have a frequency higher than the inertial frequency. Waves with exactly the inertial frequency in the deep oceans could be nonlocally excited modes that have their turning latitude at the point where measurements are being made. Equation (37) and Figure 15 do not describe such modes.

b. Vertically trapped modes. The previous section concerned modes with positive equivalent depths. The associated eigenfunctions do not form a complete set. Consider, for example, the positive equivalent depth modes associated with a positive value k and a frequency σ. Such an eastward propa-

gating disturbance excites an infinite number of inertia-gravity waves and possibly a single Kelvin wave. This infinite set of eigenfunctions is not complete because they are all exponentially small beyond the inertial latitude for the frequency σ. It follows that these functions cannot represent a forcing function that extends beyond the inertial latitude. Modes with negative equivalent depths are necessary for completeness. At subinertial frequencies these forced modes are as important as the free modes (Rossby waves): if the forcing is in the unshaded region of Figure 2, only forced modes play a role; if the forcing is in the shaded region, which occupies a very small area of the σ-s plane, then the eigenfunctions consist of a finite number of Rossby modes plus an infinite set of forced modes.

The forced modes, unlike the free modes, are not solutions of the homogeneous (unforced) equations of motion and do not correspond to natural modes of the ocean. For the most complete description of the properties of these modes, the reader is again referred to *Longuet-Higgins* [1968]. The eigenfunctions associated with the negative equivalent depth modes are, in general, oscillatory poleward of a certain turning latitude and exponentially decaying equatorward of this latitude. This is clearly evident from the equation for the special case of forcing that is independent of longitude ($s = 0$):

$$\left(\frac{d^2}{d\mu^2} + \epsilon \frac{\lambda^2 - \mu^2}{1 - \mu^2}\right) V^* = 0 \tag{38}$$

Since the free modes on the other hand are oscillatory (exponentially decaying) equatorward (poleward) of the turning latitude, the sets of eigenfunctions that correspond to the free and forced modes complement each other perfectly. Because they are trapped at the poles, the eigenfunctions with negative equivalent depths are most useful in the study of the response of high-latitude oceans. They are not particularly useful in

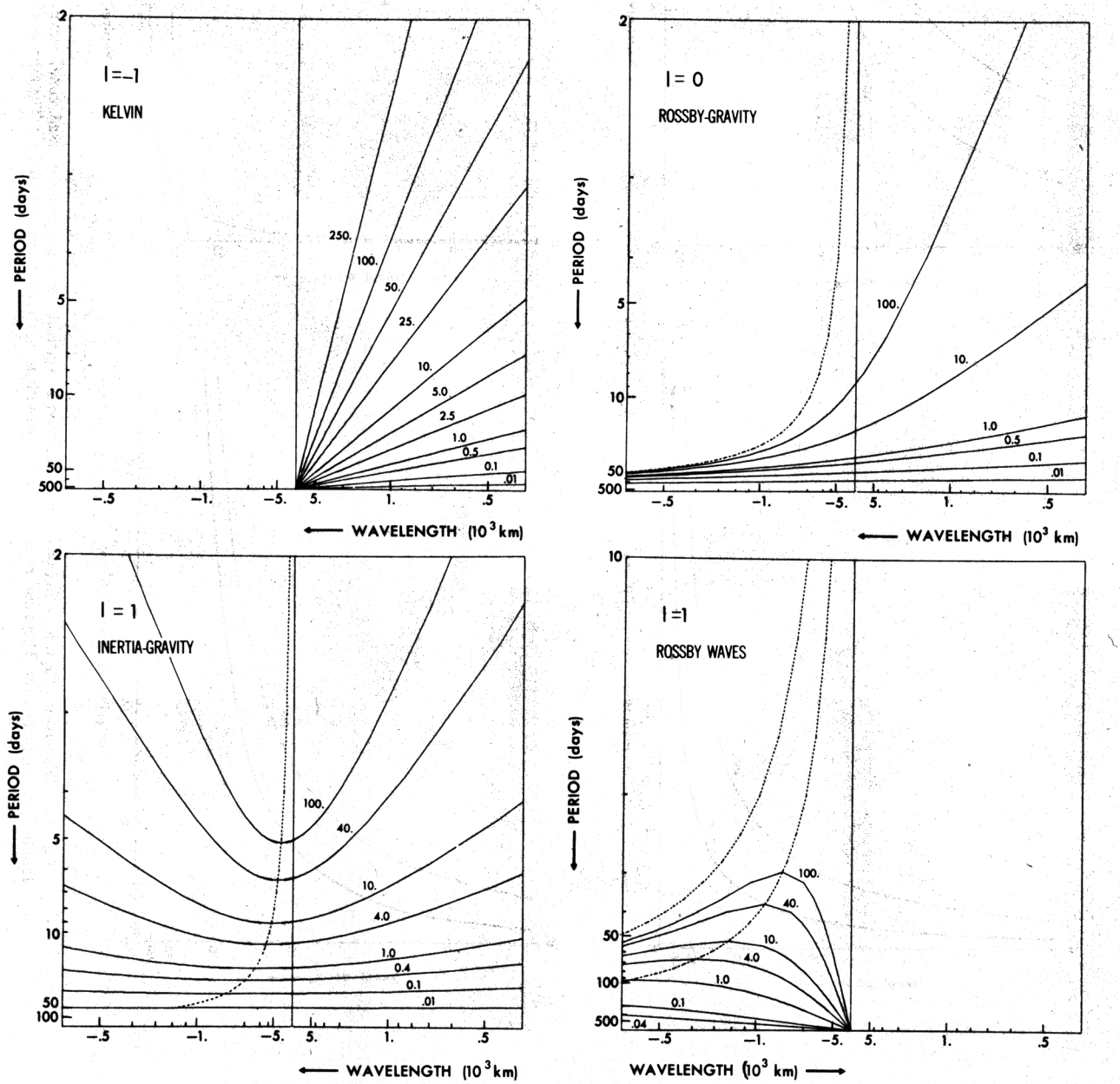

Fig. 13. Isolines of equivalent depths (in centimeters) as a function of frequency and zonal wave number for the four gravest equatorial modes.

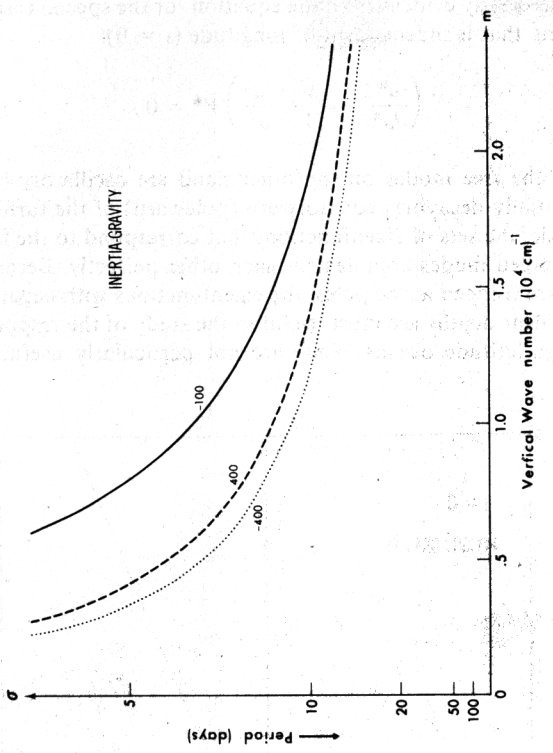

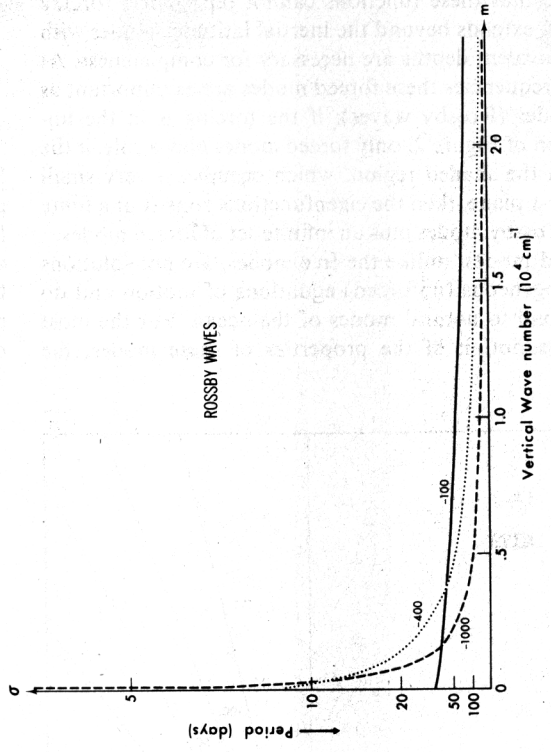

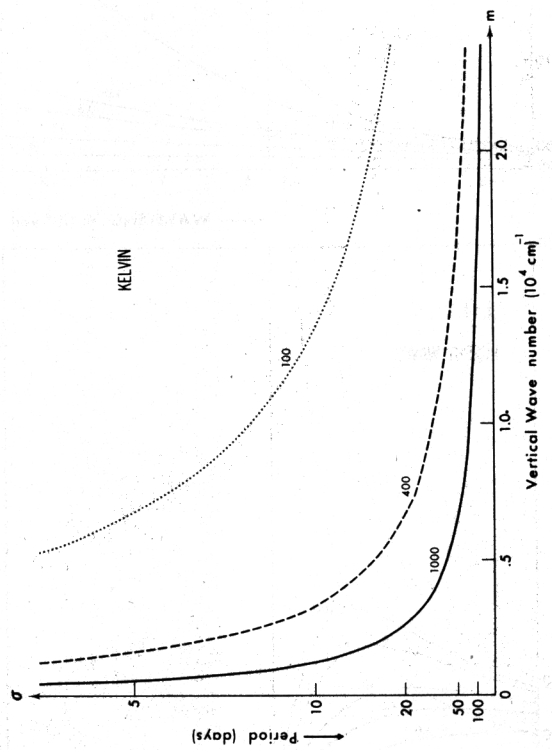

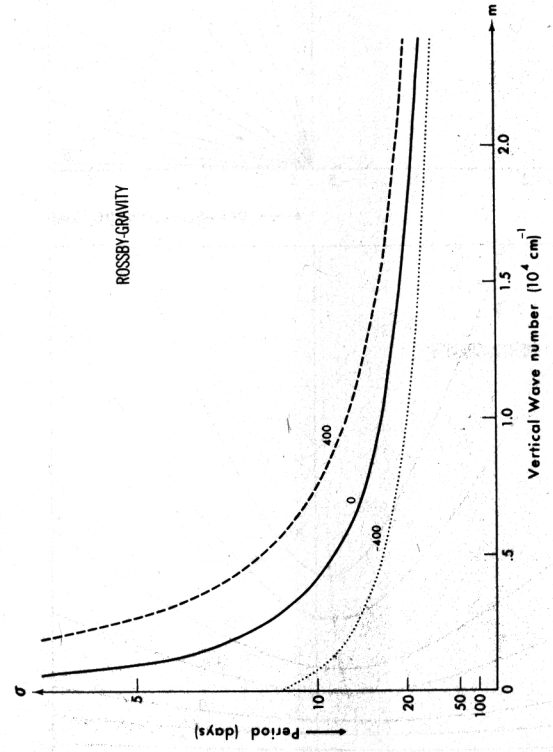

Fig. 14. Dispersion diagrams—frequency as a function of vertical wave number for fixed zonal wave numbers—for the four gravest equatorially trapped waves. These curves are based on (28) with $m = N/(gh)^{1/2}$ and $N = 10^{-2}\ s^{-1}$. The numbers on the curves are the values of l/k in units of kilometers.

studying equatorial oceans, since the gravest modes are exponentially small there.

The negative equivalent depth eigenfunctions are either symmetric or antisymmetric about the equator. If the eigenfunctions are exponentially small near the equator, then the only difference between these modes is that the motion in the two hemispheres is either in phase or in antiphase. In that case the eigenvalues for a pair of symmetric and antisymmetric modes have essentially the same values.

The eigenvalues, as a function of frequency, for three different zonal wave numbers, are shown in Figure 16. Figure 16*c* corresponds to the case in which the forcing is independent of longitude. The eigenvalues are seen to be practically independent of frequency if $\sigma < 0.2\Omega$. At low frequencies the eigenvalues come in pairs that correspond to the symmetric and antisymmetric modes referred to above. The eigenvalues of the pairs coalesce as the frequency increases, or as the (meridional) mode number increases, in agreement with the discussion in the above paragraph.

If the forcing is eastward ($s > 0$, Figure 16*a*), then the negative equivalent depths have a maximum value at a certain frequency σ_0. The negative equivalent depths become very small when the frequency is very low or very high in comparison to σ_0. This implies that the depth of penetration of the oceanic response to eastward forcing gets smaller as the frequency decreases or increases (in relation to a certain value). The depth of penetration of the response can also be shown to decrease as the horizontal dimensions of the forcing decrease.

Consider next westward propagating disturbances. The frequencies for which $h \to +\infty$ in Figure 9*b* and $h \to -\infty$ in Figure 16*b* are the same and are given by (B9) in the limit $\epsilon \to 0$. (Figure 2 shows the variation of these frequencies with zonal wave numbers for the gravest modes.) It is evident from a comparison of Figures 16*b* and 9*b* that above a certain fre-

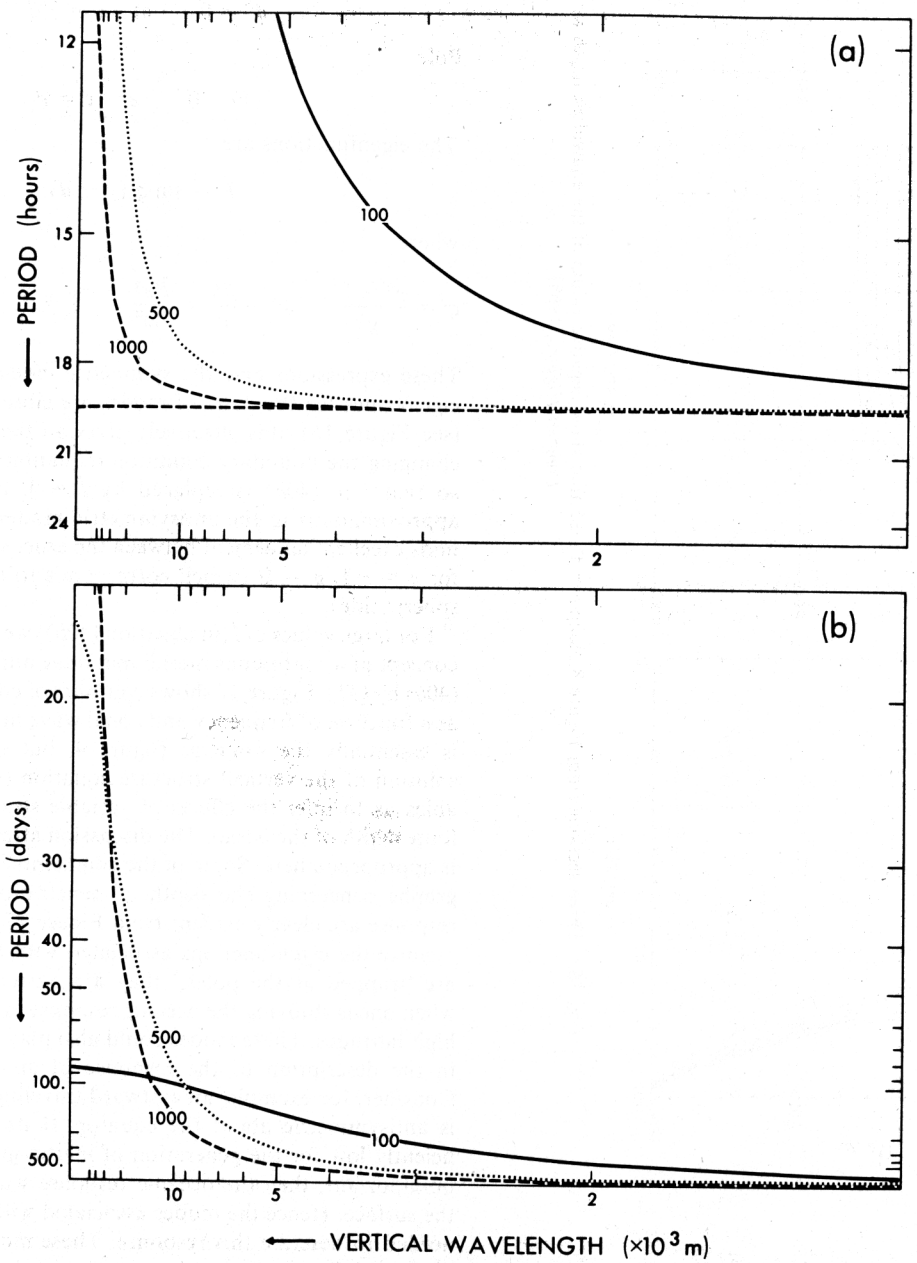

Fig. 15. Frequency as a function of vertical wave number for different fixed values of $k = l\,(\text{km}^{-1})$ for (*a*) inertia-gravity waves and (*b*) Rossby waves, according to (37), with $m = N/(gh)^{1/2}$ and β evaluated at 40°N.

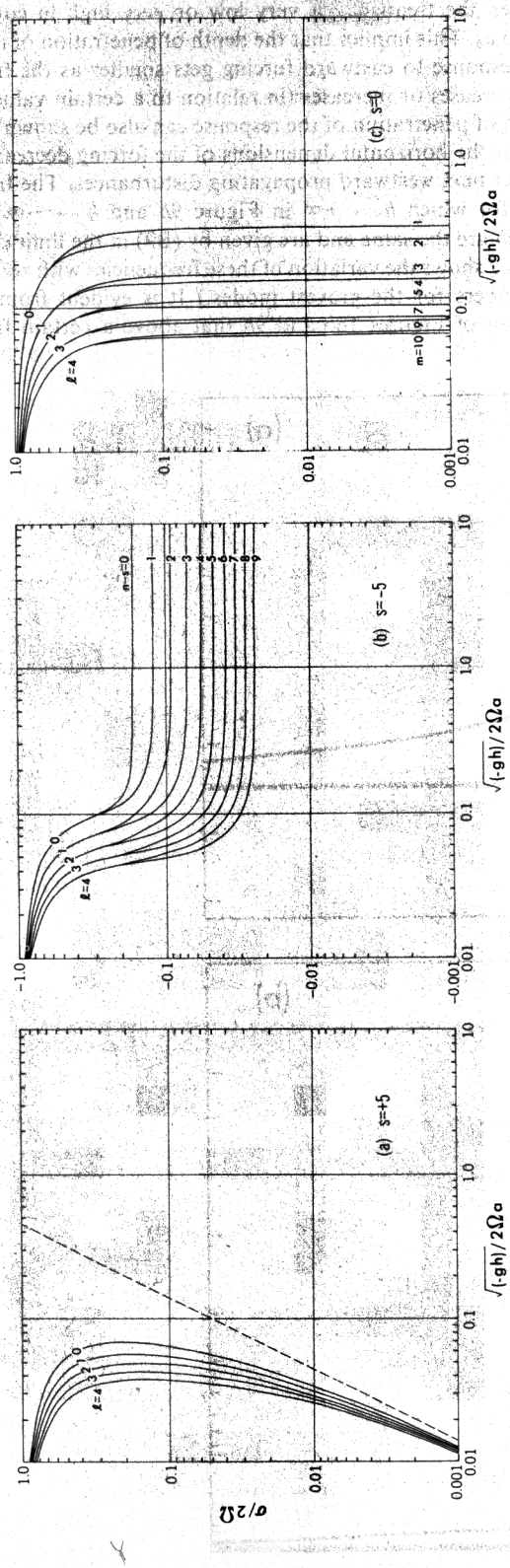

Fig. 16. Three sections from Figure 8 along $s = 0, \pm 5$ that show negative values of the equivalent depth as a function of frequency [after *Longuet-Higgins*, 1968].

quency ($\Omega/10$ for the case $s = -5$), only an infinite set of negative equivalent depth modes come into play, that is, no Rossby waves are excited. This happens if the forcing is above the shaded region of Figure 2. All the eigenvalues are finite in this case. Once the forcing is in the shaded region, fewer forced modes, but still an infinite number, plus a finite number of free modes (a perfect complement of the number of forced modes) are involved. The equivalent depths can now have infinitely large values. The likelihood of large values for the equivalent depths increases as the frequency decreases. From the discussion of the previous section, such large values for $|h|$ imply an oceanic response that is independent of depth (barotropic).

Lindzen [1967] has proposed that the negative equivalent depth modes can be approximated on a mid-latitude β plane, centered on, say, 45°N. The appropriate equation is (11), and the boundary conditions are the following:

Equator

$$V = 0 \qquad \text{at} \quad y = -d \tag{39a}$$

Pole

$$V = 0 \qquad \text{at} \quad y = d \tag{39b}$$

The eigenfunctions are

$$V = \sin q\,(y - d) \tag{40a}$$

where

$$q^2 = \frac{\sigma^2 - f_0^2}{gh} - k^2 - \frac{\beta k}{\sigma} = \frac{l^2\pi^2}{4d^2} \qquad l = 1, 2, 3, \cdots \tag{40b}$$

These expressions give the symmetric modes only. Since the eigenvalues for the pairs of modes are close together anyway (see Figure 16), this effectively gives all the eigenvalues. (By changing the boundary condition (equation (39*a*)) to $V_y = 0$ so that l in (40*b*) is replaced by $l + \frac{1}{2}$, one can calculate approximations to the antisymmetric modes.) *Lindzen* [1967] finds excellent agreement between the exact solution and (40*b*) for $s = -1$, $\sigma = \Omega$ (which corresponds to the diurnal atmospheric tide).

For large values of l (in equation (40*b*)) we can introduce the concept of a continuous meridional wave number l and replace (40*b*) by (37). Figure 17 shows contours of constant values of h as a function of frequency and zonal wave number. This figure is essentially the same as Figure 4, but together with the solution of the vertical structure equation (section D1) it enables us to infer the effects of variable stratification and the finite depth of the ocean. The discussion attendant on Figure 4 is appropriate here. Some of the comments in the above paragraphs concerning the depth of penetration of the oceanic response are clearly evident from Figure 17.

Since the eigenfunctions associated with $h < 0$ eigenvalues are 'trapped at the poles,' they are particularly convenient when one is studying the oceanic response in mid-latitudes and high latitudes. These modes could also play an important role in the description of the response of an equatorial ocean. Consider, for example, an eastward traveling disturbance that is antisymmetric about the equator. If its frequency is sufficiently low for the generation of inertia-gravity waves to be unimportant, then the oceanic response will be trapped near the surface. Hence the modes associated with $h < 0$ values are needed to describe this response. These modes, however, are exponentially small near the equator, so this method of solution is essentially a useless one for problems of this type.

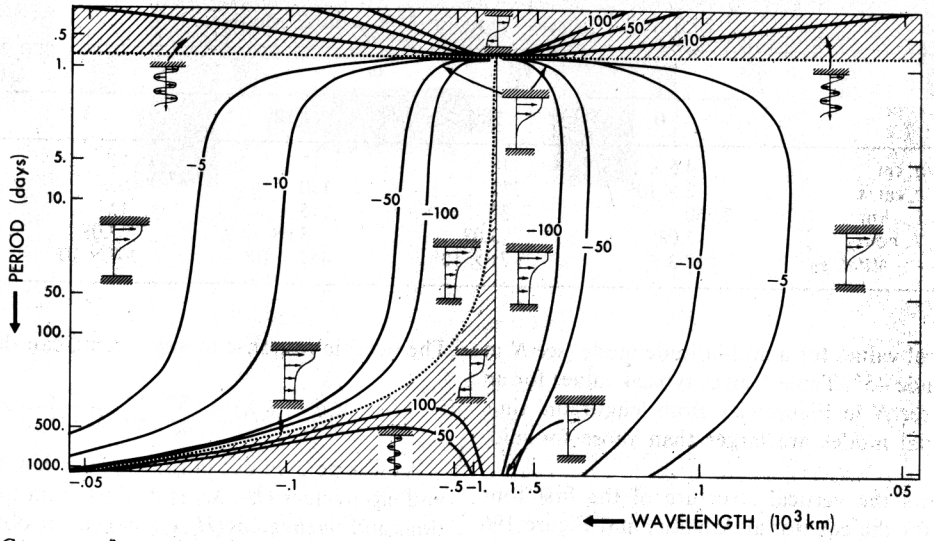

Fig. 17. Contours of constant values of h, as a function of frequency and zonal wave number, as given by (37), with f and β evaluated at 40°N. The insets show the vertical structure schematically.

E. Solutions in Terms of Vertical Baroclinic Modes

In this section we solve (1) by first solving the vertical structure equation (equation (8)) subject to the boundary conditions of (9) at the free ocean surface and rigid ocean floor. These boundary conditions cause the vertical wave numbers to be discretized so that this approach does not readily give information about vertically propagating or vertically trapped phenomena. The analysis of section D shows how the vertical modes are established by vertically propagating waves. Hence from a physical point of view, modes are possible only if the frequency is higher than inertial or if the values of σ and k fall in the shaded area of Figure 2. The vertical modes that satisfy (8) and (9), however, form a complete set and can be used to describe the oceanic response even when no free waves are excited.

1. *Vertical Modes*

Equations (8) and (9) can be solved analytically if N is constant (the vertical modes are then trigonometric functions) or if N is an exponential function (the vertical modes are then Bessel functions). *Lighthill* [1969] describes a method to calculate the modes if the density field is approximated by a number of layers each of constant density. *Munk and Phillips* [1968] note that the higher-order modes can be calculated by using the WKBJ approximation if N is nonuniform. In general, it is a trivial matter to solve the equations numerically for any $N(z)$. The equivalent depths, of the first few modes, for the equatorial and the mid-latitude stratifications are shown in Tables 1 and 2, respectively. (For the barotropic mode the equivalent depth is the actual depth of the ocean and is 4 orders of magnitude greater than the equivalent depths for the baroclinic modes.) It is clear that there can be considerable horizontal variations in the stratification $N(z)$. *Miropolskiy et al.* [1975] have discussed these variations along certain sections in the Pacific and Atlantic oceans and have also assessed the effect that the variations have on the horizontal propagation of high-frequency waves.

The characteristic speed associated with a given mode is $(gh)^{1/2}$, so that barotropic disturbances propagate several orders of magnitude faster than baroclinic disturbances. The characteristic horizontal length scale associated with a given mode is the Rossby radius of deformation

$$L_R = c/f = (gh)^{1/2}/f \tag{41a}$$

This length scale increases as the equator is approached. Outside the tropics, L_R can be evaluated locally by using the local (constant) value of f. In the tropics we define L_R such that

$$L_R = c/(f_0 + \beta L_R) \tag{41b}$$

so that

$$L_R = (c/\beta)^{1/2} \tag{41c}$$

at the equator. The latitudinal variation of L_R for a fixed value of c is shown in Figure 18. A characteristic time scale for each mode is

$$T = L_R/c \tag{42a}$$

Outside equatorial regions,

$$T = 1/f \tag{42b}$$

In equatorial regions,

$$T = 1/(\beta c)^{1/2} \tag{42c}$$

TABLE 1. Typical Values for Equatorial Modes

	m			
	0	1	2	3
h, cm	4×10^5	60	20	8
c, cm/s	2×10^4	240	140	89
L_R, km	3,100	330	250	200
T, days	0.16	1.5	2.0	2.6
$\epsilon = 4\Omega^2 a^2/gh$	17.3	129×10^3	389×10^3	972×10^3

TABLE 2. Typical Values for Mid-Latitude Modes

	m			
	0	1	2	3
h, cm	4.5×10^5	110	17	11
c, cm/s	2×10^4	332	130	105
L_R, km	2,360	37	15	12
T, hours	3.08	3.08	3.08	3.08
$\epsilon = 4\Omega^2 a^2/gh$	17.3	71×10^3	457×10^3	707×10^3

Table 2 gives typical values for a mid-latitude mode (see N in Figure 6*b*) at latitude 45°. Table 1 gives typical values for an equatorial mode (see N in Figure 6*a*). Both length and time scales for equatorial modes are larger than those for mid-latitude modes.

Figure 19*a* shows the vertical structure of the first four baroclinic modes for the equatorial Atlantic, and Figure 19*b* that for the North Atlantic. (The equivalent depths are given in Tables 1 and 2.) The barotropic mode (not shown in Figure 19) has horizontal velocity components that are practically independent of depth and a vertical velocity that decreases linearly with depth.

The complete set of eigenfunctions and eigenvalues (i.e., barotropic plus baroclinic modes and equivalent depths) will be denoted by $\{Z_m, \epsilon_m\}$. All the ϵ_m and equivalent depths are positive. Here m is the signature of the mode and represents the number of nodes that a mode has between ocean floor and ocean surface. (The continuous range of vertical wave numbers of section D has been discretized.) This complete set of functions can be used to represent the vertical structure of any forcing function (provided it is a body force). *Lighthill* [1969] asserts that all but the barotropic and first two baroclinic modes can be disregarded, but *Moore and Philander* [1976] have pointed out that the validity of this statement strongly depends on the stratification and on the depth of the mixed layer in which the body force acts. The discussion of the previous section shows that there are situations in which a very large number of vertical modes may be necessary to describe the oceanic motion. The frequency and zonal wave number of the forcing are of critical importance.

2. *Latitudinal Structure of the Solution*

Now that the vertical structure of the solution has been determined, it remains to solve equation (10), with the appropriate component of the forcing term on the right-hand side, for each mode. One way to proceed is to determine the eigenvalues of the homogeneous equation (10), with λ regarded as the eigenvalue. (The values of ϵ_n, all of which are positive, are known, since the equivalent depths are known from the solution of (8).) This complete set $(\bar{H}_l, \lambda_l)$ can be used to expand the forcing function in a series:

$$F(\theta, z, s, \lambda) = \sum_m \sum_l A_{lm} Z_m(z) \bar{H}_l(\theta) \qquad (43)$$

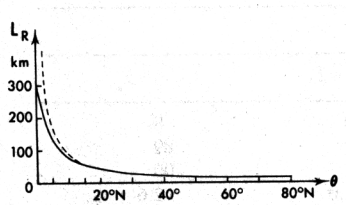

Fig. 18. Variation of the radius of deformation with latitude, according to equation (41*b*), for the first baroclinic mode. (The dotted curve is (41*a*).)

The oceanic response to any forcing can then be written

$$V(\theta, z, s, \lambda) = \sum_m \sum_l \frac{A_{lm}}{\lambda - \lambda_{lm}} Z_m(z) \bar{H}_l(\theta) \qquad (44)$$

As was pointed out in the introduction, the set of functions and eigenvalues $(\bar{H}_l, \lambda_l)$ is distinct from the set of eigenfunctions and eigenvalues (H_l, ϵ_l) that can be obtained from (10) by treating ϵ_l as the eigenvalue. Both sets of eigenvalues will of course satisfy the same dispersion relation (equation (23)). Whereas we determine h, for given σ and k, from (23) in section D, we are now interested in the relation between σ and k for given positive values of h.

For the baroclinic modes of the ocean, which have large values of ϵ (see Table 2), the gravest latitudinal modes are equatorially trapped and are accurately described by equation (13). It is convenient to nondimensionalize the variables with respect to the length and time scales of (41*c*) and (42*c*):

$$(x, y, 1/k) = \left(\frac{c}{\beta}\right)^{1/2} (\xi, \eta, 1/\bar{k}) \qquad \left(t, \frac{1}{\sigma}\right) = \frac{1}{(\beta c)^{1/2}} (\tau, 1/\bar{\sigma})$$

Then (11) becomes

$$V_{\eta\eta} + [\bar{\sigma}^2 - \bar{k}^2 - (\bar{k}/\bar{\sigma}) - \eta^2]V = F_m(\eta, \bar{k}, \bar{\sigma}) \qquad (45)$$

where F_m is the projection of the forcing function onto the baroclinic mode under consideration. The advantage of this formulation is that the homogeneous part of (45) is exactly the same for each baroclinic mode. Equation (45) satisfies the condition of boundedness at large values of η provided

$$\bar{k}^2 + (\bar{k}/\bar{\sigma}) - \bar{\sigma}^2 + 2l + 1 = 0 \qquad (46)$$

This is merely a nondimensional version of (27), but we now regard it as an equation for $\bar{\sigma}$. This cubic has three roots: two correspond to inertia-gravity waves, and the other to a Rossby wave. The solid curves in Figure 20 are the curves described by (45). This figure is a σ-k section from Figure 8. The dashed curve in Figure 20 is described by

$$\bar{k} = -1/2\bar{\sigma} \qquad (47)$$

and is the locus of zero group velocity points. The modes (eigenfunctions) are described by Hermite functions [*Matsuno*, 1966] (see Appendix A). Individually, each latitudinal mode is physically the same as the modes discussed in section D2, but the two sets of modes are distinct. For example, the set discussed in section D satisfies the orthogonality relation (equation (30)). The set under discussion here satisfies the relation (equation (A4)) in Appendix A. Figure 21 shows the latitudinal structure of the first few modes given by (45) with $\bar{\sigma}$ as eigenvalue. This is to be contrasted with the modes shown in Figures 11 and 12. Here the Rossby and inertia-gravity modes of the same order l are described by the same Hermite function. The latitudinal scale for these functions is the radius of deformation. As the order l of the mode increases, the turning latitudes steadily increase. This set of Hermite functions is

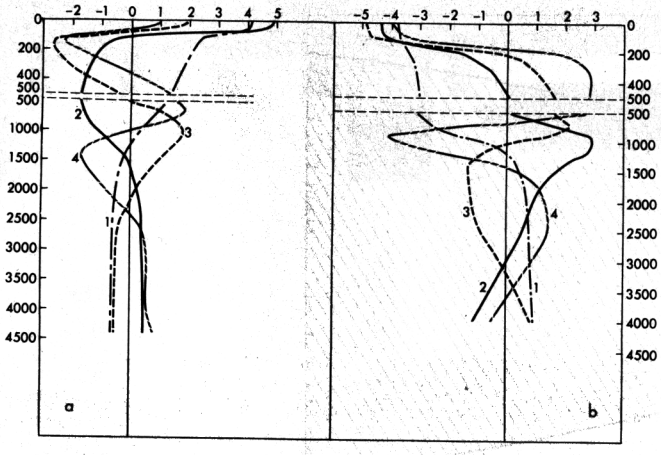

Fig. 19. Structure of the vertical baroclinic modes for (*a*) the equatorial and (*b*) mid-latitude stratification shown in Figure 6. The equivalent depths are given in Tables 1 and 2.

complete on an infinite equatorial β plane [*Cane and Sarachik*, 1976]. (This is not true of the set discussed in section D.)

There is, in addition to the modes given by (45), a Kelvin wave for which $V \equiv 0$ on an equatorial β plane. This mode is described by (25) and (26), where h has the appropriate value for the mode under consideration.

If the frequency and wave number of the forcing should be such that (46) is satisfied, then a resonant mode of the ocean will be excited. Thus if an atmospheric storm has energy over a wide band of frequencies and wave numbers, then the spectrum of the oceanic response will have peaks at frequencies and wave numbers that satisfy (46). The largest peak will occur at those frequencies for which the zonal group velocity vanishes, for at other frequencies the energy will disperse. Hence for a given baroclinic mode, strong resonance will occur at the frequencies corresponding to the intersection of the solid curves and the dashed curve in Figure 20. *Wunsch and Gill* [1976] have explained peaks in sea surface height spectra from islands in the equatorial Pacific in this manner. We re-examine this hypothesis in section H.

If the forcing is nonresonant, then the solution can be expressed in terms of the modes, as is described above. This

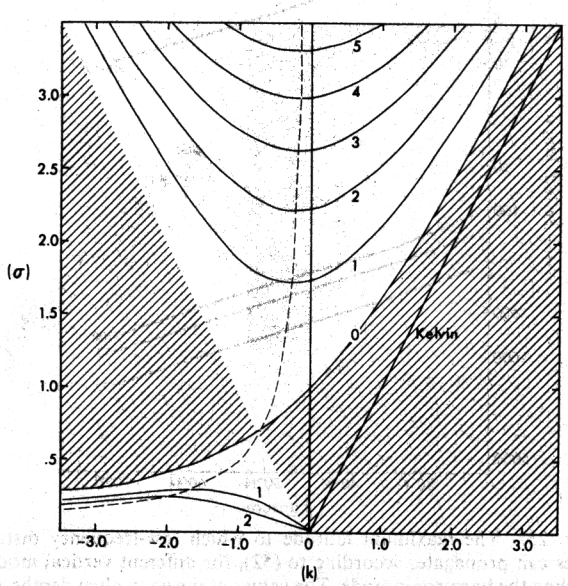

Fig. 20. The dispersion diagram for equatorial waves according to (46). This figure is a section, in the σ-k plane, from Figure 8.

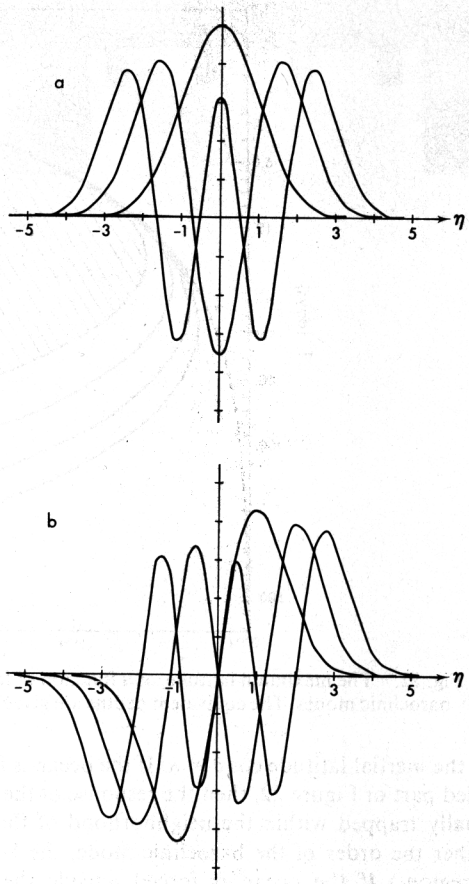

Fig. 21. The gravest (*a*) symmetric and (*b*) antisymmetric eigenfunctions for the homogeneous equation (45).

approach has been adopted in numerous studies. (See, for example, *Cane and Sarachik* [1976] and references therein.) An alternative procedure is to calculate the Green function of (46). (It can readily be expressed in terms of parabolic cylinder functions of noninteger order.) This representation of the solution is more informative and compact than the other one if the forcing function has energy over a band of frequencies and wave numbers for which no natural modes of the ocean are excited (i.e., if the Fourier transform of the forcing function falls entirely outside the shaded region of Figure 2). Inspection of (45) reveals that for point forcing near the equator the response will decay exponentially beyond a latitude

$$\eta_T = (\bar{\sigma}^2 - \bar{k}^2 - \bar{k}/\bar{\sigma})^{1/2} \tag{48}$$

For $\bar{\sigma}$, $\bar{k}$ values in the shaded part of Figure 20 the above expression gives zero or imaginary values of η, in which event the response to forcing at a point is only felt a latitudinal distance $\eta = O(1)$, a distance equal to the radius of deformation, from that point. Along the solid lines in Figure 20 the disturbances are felt a distance

$$\eta_T = (2l + 1)^{1/2} \qquad l = 0, 1, 2, \cdots \tag{49}$$

from the equator.

A disturbance will propagate furthest from the equator if its zonal wave number falls on the dashed curve of Figure 20. In that case,

$$\eta_{\max}{}^2 = (1/4\bar{\sigma}^2) + \bar{\sigma}^2 \tag{50}$$

Figure 22 shows $\eta_{\max}$ as a function of frequency for the first four baroclinic modes of Table 1. The dashed curve in this

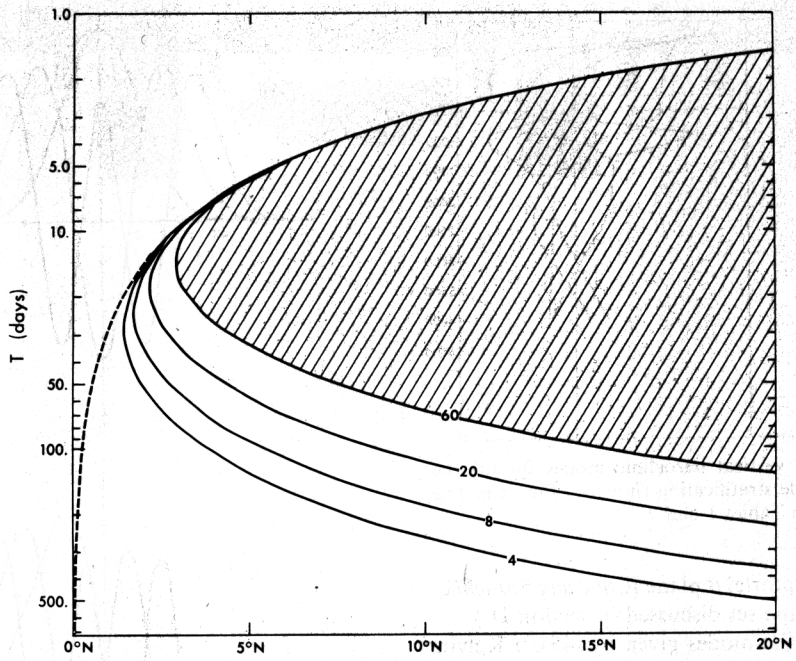

Fig. 22. The maximum latitude, as a function of frequency, to which equatorial disturbances can propagate for different baroclinic modes. The equivalent depths are given (in centimeters) on the curves. The dashed curve is the inertial latitude.

figure is the inertial latitude $\cos\theta = \lambda$. If the ocean is forced in the shaded part of Figure 22, then the response of the ocean is latitudinally trapped within the neighborhood of the region. (The higher the order of the baroclinic mode, the larger the shaded region.) If the ocean is forced outside the shaded region, then disturbances with a given frequency can propagate poleward as far as the turning latitude for that frequency. (The turning latitude is the boundary between the shaded and the unshaded region.) We note that the (high frequency) inertia-gravity waves can propagate further than the inertial latitude, but as the frequency increases, the turning latitudes for all the baroclinic modes become asymptotic to the inertial latitude. (In section C we showed that vertically propagating inertia-gravity waves of sufficiently large meridional wave number all have their turning latitudes at the inertial latitude.) This is the basis for the hypothesis of *Munk and Phillips* [1968] that the peak in the oceanic spectrum at the local inertial frequency is due to the nonlocal (global) generation of these waves. We return to this matter in section H.

It is clear from Figure 22 that the low-frequency Rossby waves also have turning latitudes. These are weaker condensation points than those associated with inertia-gravity waves, because for Rossby waves each baroclinic mode has a different turning latitude. *Longuet-Higgins* [1965] and *Blandford* [1966] explain subinertial frequency eddies near Bermuda [*Swallow*, 1961] as nonlocally generated Rossby waves that have reached their turning latitude.

The discussion thus far has concerned the latitudinal dispersion of energy. For wide ranges of frequency, which increase with increasing latitude, the response of the ocean is latitudinally trapped. In such cases the response is also trapped in longitude. Consider equation (11), nondimensionalized according to (41) and (42):

$$V_{\xi\xi} + V_{\eta\eta} + (i/\sigma)V_\xi + (\bar{\sigma}^2 - \eta^2)V = 0$$

Write

$$V = \tilde{V}e^{-i\xi/2\bar{\sigma}}$$

Then

$$\tilde{V}_{\xi\xi} + \tilde{V}_{\eta\eta} + Q\tilde{V} = 0 \qquad (51a)$$

where

$$Q = (1/4\bar{\sigma}^2) + \bar{\sigma}^2 - \eta^2 \qquad (51b)$$

If $Q > 0$, then (51) permits solutions that are oscillatory in ξ and η so that waves can propagate across circles of latitude and longitude. (The poleward propagation is possible only up to the turning latitude where $Q = 0$.) If the frequency of the forcing is such that $Q < 0$, then it can be shown (with considerable effort) that the Green function for (50) in an unbounded

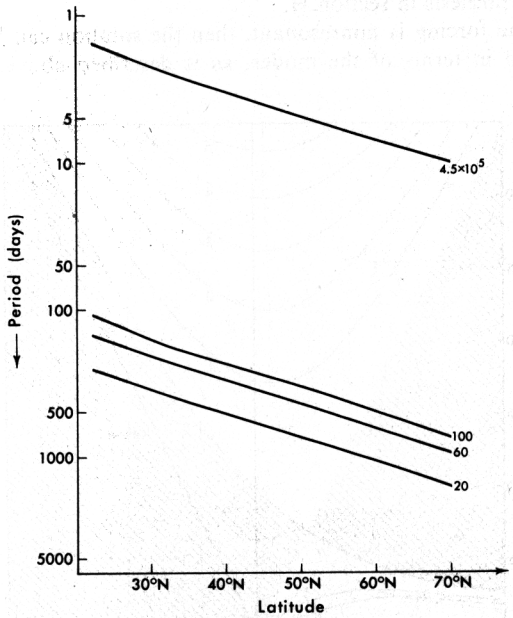

Fig. 23. The maximum latitude to which low-frequency disturbances can propagate, according to (52), for different vertical modes including the barotropic mode. The values of the equivalent depths are given in centimeters.

region is exponentially decaying in both horizontal directions. Alternately, note that when $Q < 0$, solutions of (51) must be exponentially decaying in at least one direction. Physically, this can only happen with increasing distance from a wave guide. Coasts provide such a wave guide for Kelvin waves. We conclude that if the frequency of the forcing is such that $Q < 0$ and if we are not in the neighborhood of coasts, then the oceanic response decays exponentially with distance from the forcing region.

The turning latitude given by (51*b*) is identical to that given by (50). Hence in the shaded region of Figure 22 the baroclinic response is trapped in both latitude and longitude.

The validity of the equatorial β plane ($f = \beta y$) is limited to the tropics. Since the turning latitudes of the modes $\tilde{H}_l$ described above increase as l increases (see (49) and Figure 21), mid-latitude modes are associated with high values of l. The spheroidal wave equation (equation (12)) is a good approximation to Laplace's tidal equations at large values of l. (See Appendix B.) An analysis of this equation shows that for Rossby waves the turning latitude θ is given by the equation

$$(s^2 - \tfrac{1}{4})\operatorname{cosec}^2\theta + \epsilon\cos^2\theta + (2/\lambda) - \tfrac{1}{4} = 0 \qquad (52)$$

The turning latitude is a maximum when

$$s = -\sin^2\theta/2\lambda \qquad (53)$$

(This equation is the same as (47) in the tropics provided s is large.) The maximum turning latitude is shown as a function of frequency in Figure 23 for the barotropic and first few baroclinic modes.

The above results can be obtained in an approximate form from the β plane equations in a manner similar to that described in section D and Appendix B. The mid-latitude, β plane approximation version of (51), with $f_0 = \text{const}$, is

$$\tilde{V}_{\xi\xi} + \tilde{V}_{\eta\eta} + [(\alpha/4\tilde{\sigma}^2) + \tilde{\sigma}^2 - 1]\tilde{V} = 0 \qquad (54)$$

where the nondimensionalization is now according to (41*a*) and (42*b*) and $\alpha = \beta L_R/f_0$. At 45°N, $\alpha = L_R/a$ is the ratio of the radius of deformation to the radius of the earth, so this term in (54) is important at low frequencies only. The Green function for this equation is

$$G = \frac{1}{2\pi}K_0(QR) \sim \frac{1}{2\pi}\left(\frac{\pi}{2QR}\right)^{1/2} e^{-QR} \qquad \text{for large } R$$

where R is the radial distance from the point source (ξ_0, η_0) and

$$Q^2 = 1 - \tilde{\sigma}^2 - (\alpha/4\tilde{\sigma}^2)$$

For a wide range of subinertial frequencies, $Q^2 = 1$, so the oceanic response decays exponentially from the point force with an e folding distance equal to the radius of deformation. For frequencies close to the inertial frequency the e folding distance becomes very large. This result, which is inconsistent with the results in Figure 4, is correct for a constant density fluid of depth h, but the result needs to be interpreted with caution if the fluid is stratified. What we in effect have done here is to interpret the dispersion relation

$$gh = (\sigma^2 - f_0^2)/(k^2 + l^2 + \beta k/\sigma)$$

as an equation for (negative) values of $k^2 + l^2$, after a positive value for h had been specified. But we know from section D that h can assume negative values for a stratified fluid. This tells us that when the (vertical) modal description is used, care must be taken to use a sufficiently large number of vertical modes to describe the vertical structure. As the frequency approaches the inertial frequency and the response becomes more vertically trapped, a larger and larger number of vertical modes are necessary. In the limit $\sigma \to f$ the modal description breaks down. An approach such as that used in section B (see Figure 4) may be more useful than an analysis based on vertical modes.

In the limit of very large equivalent depths ($\epsilon \to 0$) there are only two classes of modes: inertia-gravity waves and Rossby waves. (In the transition $\epsilon = \infty$ to $\epsilon = 0$ the Kelvin wave becomes an inertia-gravity wave, and the Rossby-gravity wave a Rossby wave [*Longuet-Higgins*, 1968; *Golitzyn and Dikii*, 1966]. The equivalent depth for the barotropic mode of the oceans is large ($\epsilon \sim 20$), so it is unclear whether the gravest modes will be identifiable as Kelvin and mixed Rossby-gravity waves.

Figure 24 shows the latitudinal structure of the gravest eastward propagating symmetric mode for $\epsilon = 10$ and 100 as calculated by *Longuet-Higgins* [1968]. It clearly resembles a Kelvin wave. In the figures of Longuet-Higgins the gravest antisymmetric mode is identifiable as a Rossby-gravity wave. Hence the gravest barotropic modes are therefore similar in structure to the latitudinally gravest baroclinic modes. The tidal forcing may excite these grave modes in ocean basins that are sufficiently large (the Pacific Ocean).

F. Effects of Coastal Boundaries

There are two ways in which the effect of meridional coastal boundaries can be taken into account. One approach is to separate variables, as in section B, and to seek solutions to LTE that satisfy the boundary conditions at the coasts. The assumption that the solutions have the form e^{ikx} (or $e^{is\phi}$) must then be abandoned. *Moore* [1968] and *Longuet-Higgins and Pond* [1970] adopted this method. Alternatively, we can assume that solutions do have the form e^{ikx}, as if the ocean were unbounded. Reflected and coastally trapped waves, which are

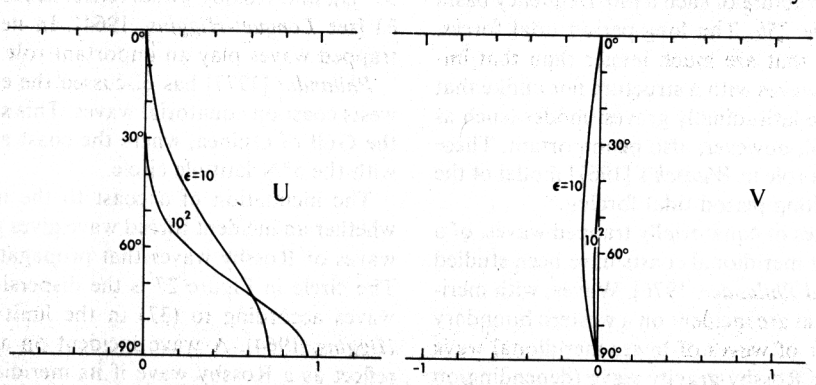

Fig. 24. The latitudinal structure of the barotropic equatorial Kelvin wave [after *Longuet-Higgins*, 1968].

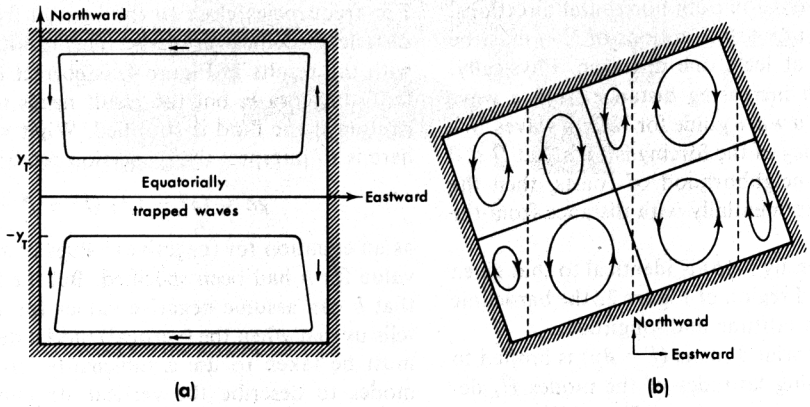

Fig. 25. (*a*) Structure of a normal mode of the ocean at a frequency close to σ_0 (see (55)). The arrows denote coastally trapped Kelvin waves [after *Moore*, 1968]. (*b*) Streamlines of a normal mode in a basin on a β plane, at frequencies much less than σ_0. The dotted lines drift westward [after *Longuet-Higgins*, 1965].

necessary to satisfy boundary conditions at the coast, can then be considered separately.

The vertical structure of the modes of a basin will of course correspond to the vertical modes described in section E1. For a certain range of frequencies centered on σ_0, where

$$\sigma_0^2 = \beta(gh)^{1/2}/2 \tag{55}$$

the horizontal structure of the modes is as shown in Figure 25*a*. (The frequency σ_0 corresponds to the point of contact of the shaded regions in Figure 20, and the horizontal dotted line in Figure 26. Numerical values for σ_0 are $2^{1/2}$ times the values given in Table 2.) According to Figure 25*a* the horizontal structure of the modes of the basin consists of equatorially trapped waves within a latitude band given by (50) or (52). Poleward of this latitude the amplitude of the modes decays exponentially except within a radius of deformation of the coast where Kelvin waves are possible. The gravest symmetric mode can be thought of as a Kelvin wave that rotates counterclockwise, in the northern hemisphere, around the basin. The period of this mode is essentially the time that it takes a Kelvin wave to complete this route. In a flat-bottomed basin with sufficiently large dimensions the diurnal tidal force will directly excite a nondivergent Rossby wave ($h = \infty$, $s = -1$). Because of the meridional coasts, there will be additional waves similar in structure to those in Figure 25*a*. (Equation (55) is approximately satisfied by the diurnal tide.)

For frequencies much lower (or higher) than σ_0 the turning latitude y_T in Figure 25*a* is close to the pole, the role of coastal Kelvin waves is unimportant, and the modes of the basin can be described in terms of nearly nondivergent Rossby (or inertia-gravity) waves. The structure of such a low-frequency basin mode is shown in Figure 25*b*. The long-period tidal forces, which have periodicities that are much longer than that implied by (55), will excite waves with a structure not unlike that shown in Figure 25*b*. The latitudinally gravest modes (such as the one in Figure 25) will, however, also be important. These grave modes are denied a role in *Wunsch*'s [1967] model of the oceanic response to the long-period tidal forcing.

The reflection properties of equatorially trapped waves, of a given baroclinic mode, at meridional coasts have been studied by Moore [see *Moore and Philander*, 1976]. Waves, with meridional wave number l, that are incident on a western boundary reflect as a finite number of waves of lower meridional wave number plus a Kelvin or Rossby-gravity wave (depending on the symmetry of the incident wave). It follows that the reflected waves are at least as equatorially trapped as the incident wave. Since the Kelvin and Rossby-gravity waves both have eastward group velocities for all frequencies, they cannot be excited at eastern boundaries which therefore have different reflection properties. The finite number of waves reflected at an eastern boundary again have lower meridional wave numbers than the incident waves, but they are not sufficient to satisfy the boundary condition $u = 0$ at the coast. In addition, an infinite number of coastally trapped Poincaré waves are necessary. At a large distance from the equator the sum of these waves can be shown to represent a poleward propagating, coastally trapped Kelvin wave [*Moore*, 1968]. The *e* folding distance, with which the amplitudes of the Poincaré waves decay from the coast, can be calculated from (46); it corresponds to solutions that have imaginary values for k and is shown in Figure 26. Except for small frequency ranges in the neighborhood of points of zero zonal group velocity the coastally trapped waves have an *e* folding distance equal to or less than a radius of deformation. The meridional structure of each of these coastally trapped modes is the corresponding Hermite function. Hence the higher the latitude, the less important are the gravest modes, and the more coastally trapped are the waves. This is equivalent to saying that the *e* folding distance of the amplitude of the coastal Kelvin wave is the radius of deformation, which decreases with increasing latitude.

Outside the tropics there is a large gap between the inertial period and the highest period of the free Rossby waves ($1/\tilde{\sigma}$, say). Forced waves, in this frequency range, that are incident on a meridional coast will excite the coastally trapped waves, but there will be no reflected waves. At the opposite extremes, inertia-gravity waves reflect as inertia-gravity waves (when $\sigma \gg f_0$), and Rossby waves reflect as Rossby waves (when $\sigma \ll \tilde{\sigma}$) [see *Longuet-Higgins*, 1964]. In neither case do coastally trapped waves play an important role.

Philander [1977] has discussed the effect of a zonal (east to west) coast on equatorial waves. This study may be relevant to the Gulf of Guinea, where the coast approximately coincides with the 5°N latitude circle.

The inclination of a coast to the meridian can determine whether an incident forced wave gives rise to coastally trapped waves or Rossby waves that propagate away from the coast. The circle in Figure 27 is the dispersion diagram for Rossby waves according to (37) in the limit $\sigma \ll f_0$ [see *Longuet-Higgins*, 1964]. A wave incident on a north-south coast will reflect as a Rossby wave if its meridional wave number falls between points A and B in Figure 27. To reflect as a Rossby wave from a coast inclined at an angle α to the meridian, the

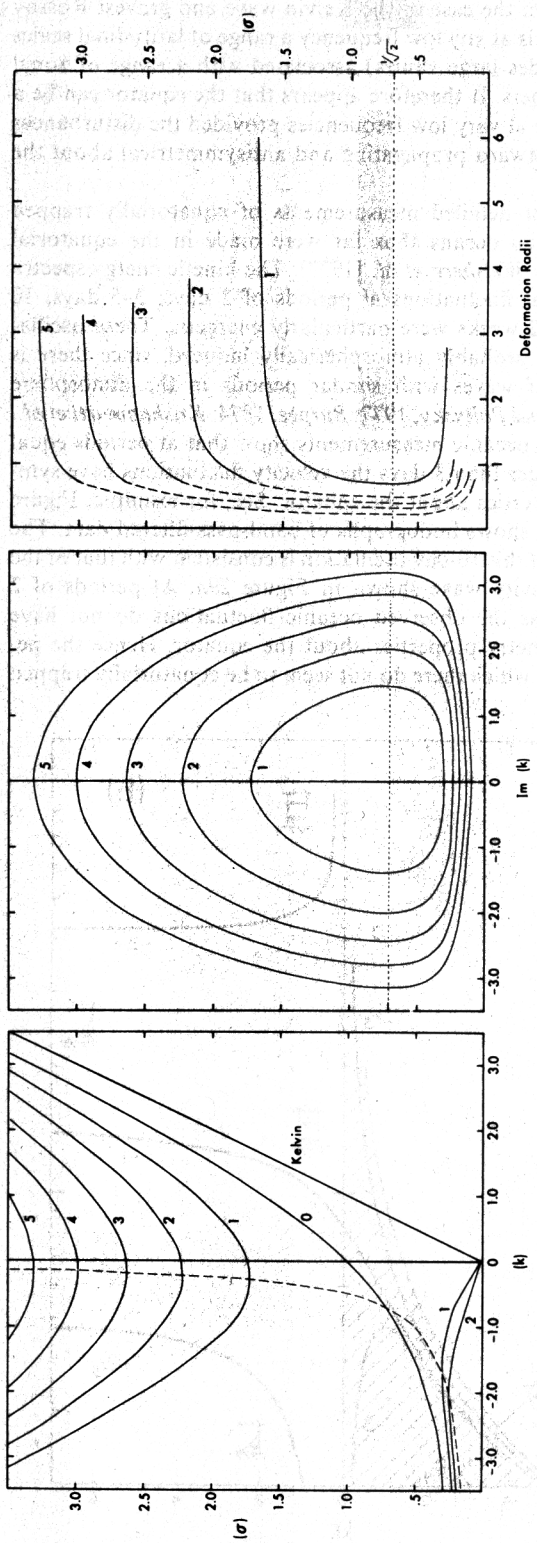

Fig. 26. The e folding distance with which the amplitude of coastally trapped waves decays, as a function of frequency for the gravest modes, $l = 1, \cdots, 5$. The results are obtained from (46) for the frequency ranges for which k has imaginary values. (These are shown in the middle figure.) The left-hand figure is the dispersion diagram of Figure 20.

meridional wave number of the incident wave must fall between points C and D. Hence if the forced wave has a meridional wave number corresponding to point E, it will give rise to coastally trapped waves along the inclined coast but to Rossby waves in the case of a north-south coast. The reflection of equatorial waves from a coast inclined to the meridian (as in the case of the eastern coasts of Africa and South America) is yet to be studied.

G. Effects of Bottom Topography

The separation of variables described in section B is, with the exception of certain special cases to be discussed shortly, possible only if the ocean floor is flat. In the case of an arbitrarily irregular ocean floor one can still proceed as in section D and study the downward propagating waves as if a radiation condition were appropriate at the bottom. The waves reflected upward could then be investigated separately. This approach is useful in the tropical Atlantic, for example, where the enormous mid-Atlantic ridge scatters waves incident on it (see section H1). Should the stratification be such that most of the energy is reflected internally before the waves reach the ocean floor, then it may be justifiable to neglect the topography altogether and to use the method of vertical baroclinic modes (see sections D1 and E).

Apart from its effect on waves incident on it, the topography plays another important role: it supports certain types of wave motion such as Stokes edge waves and topographic Rossby waves for which it provides a restoring force. *Rhines* [1970] has studied the effect of stratification on these waves when the slope of the ocean floor is linear in y (latitude). The results are summarized in Figure 28. For the frequency–wave number range, where vertically propagating Rossby waves are possible, i.e., the shaded parts of Figures 17 and 28, the slope of the ocean floor now permits vertical modes different in structure from those described in section E. In the frequency–wave number range, where previously, no freely propagating Rossby waves were possible, i.e., the unshaded parts of Figures 17 and 28, it is now possible to have waves that propagate freely in the horizontal. These waves, however, do not propagate vertically; their amplitudes attenuate with increasing distance from the ocean floor. The e folding distance is so large for long westward propagating waves that they are essentially barotropic. For short waves, and for long low-frequency eastward propagating waves, the e folding distance is small, and the waves are bottom trapped. (Eastward traveling waves are possible if the slope of the ocean floor negates the β effect.)

In a flat-bottomed ocean, large eastward traveling storms force a nonresonant (and therefore a fairly mild) response. The effect of these large storms penetrates to the ocean floor. It is therefore possible for them to excite bottom-trapped waves resonantly if the topography can support such waves. In other words, topographic features can significantly alter the oceanic response to forcing. Note that bottom-trapped waves with short horizontal scales cannot be excited directly by small-scale disturbances at the surface. The response to small storms (fronts) is strongly trapped in the vertical.

H. Implications

1. *Equatorially Trapped Waves*

The oceanic response to forcing can always be described in terms of latitudinal modes (as in section D), but we do not expect these modes to be established in the ocean except under restricted conditions. For example, an atmospheric storm in

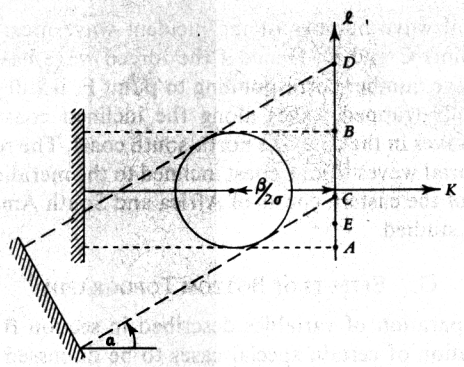

Fig. 27. The circle is the locus of points that satisfy the dispersion relation (equation (37)) when $\sigma \ll f_0$. Its radius is $[(\beta^2/4\sigma^2) - (f^2/gh)]^{1/2}$.

the vicinity of 30°N will excite inertial waves with a period of 1 day, but the latitudinal structure of these waves is unlikely to correspond to a Hough function that spans the latitude band 30°N to 30°S. Disturbances near the equator, on the other hand, are likely to excite the gravest equatorially trapped modes. The equivalent depth h of a mode is a measure of its latitudinal scale. The larger the value of h, the larger is the latitudinal scale, and the less likely is the establishment of the associated mode. Figure 13 shows that at high frequencies the (latitudinally) gravest modes have large equivalent depths (except for short Kelvin waves). This suggests that the equator is unlikely to be a wave guide at high frequencies (except possibly for Kelvin waves). At very low frequencies, on the other hand, the gravest inertia-gravity waves and the Rossby-gravity wave have small values for h and are strongly trapped about the equator. Indeed, their latitudinal scales become so small that the implied latitudinal shears are too large for these waves to be stable. In the case of the Kelvin wave and gravest Rossby wave there is at any low frequency a range of latitudinal scales (that includes large values) associated with a range of zonal wave numbers. It therefore appears that the equator can be a wave guide at very low frequencies provided the disturbances are not eastward propagating and antisymmetrical about the equator.

The most detailed measurements of equatorially trapped waves in the oceans thus far were made in the equatorial Atlantic by *Weisberg et al.* [1977]. The kinetic energy spectra suggest that fluctuations at periods of 2 days, 3–5 days, 10 days, and 2 weeks were particularly energetic. These oscillations were probably atmospherically induced, since there is evidence of waves with similar periods in the atmosphere [*Orlanski and Polinsky*, 1977; *Burpee*, 1974; *Krishnamurti et al.*, 1975]. The oceanic measurements show that at periods equal to and longer than 3 days the velocity fluctuations have symmetry properties about the equator. See, for example, Figure 29*b*, which shows hodographs of band-pass-filtered data. The structure of this 10-day oscillation is consistent with that of the Rossby-gravity wave shown in Figure 29*a*. At periods of 2 days or less the observed oceanic fluctuations do not have these symmetry properties about the equator. Hence the period below which there do not seem to be equatorially trapped

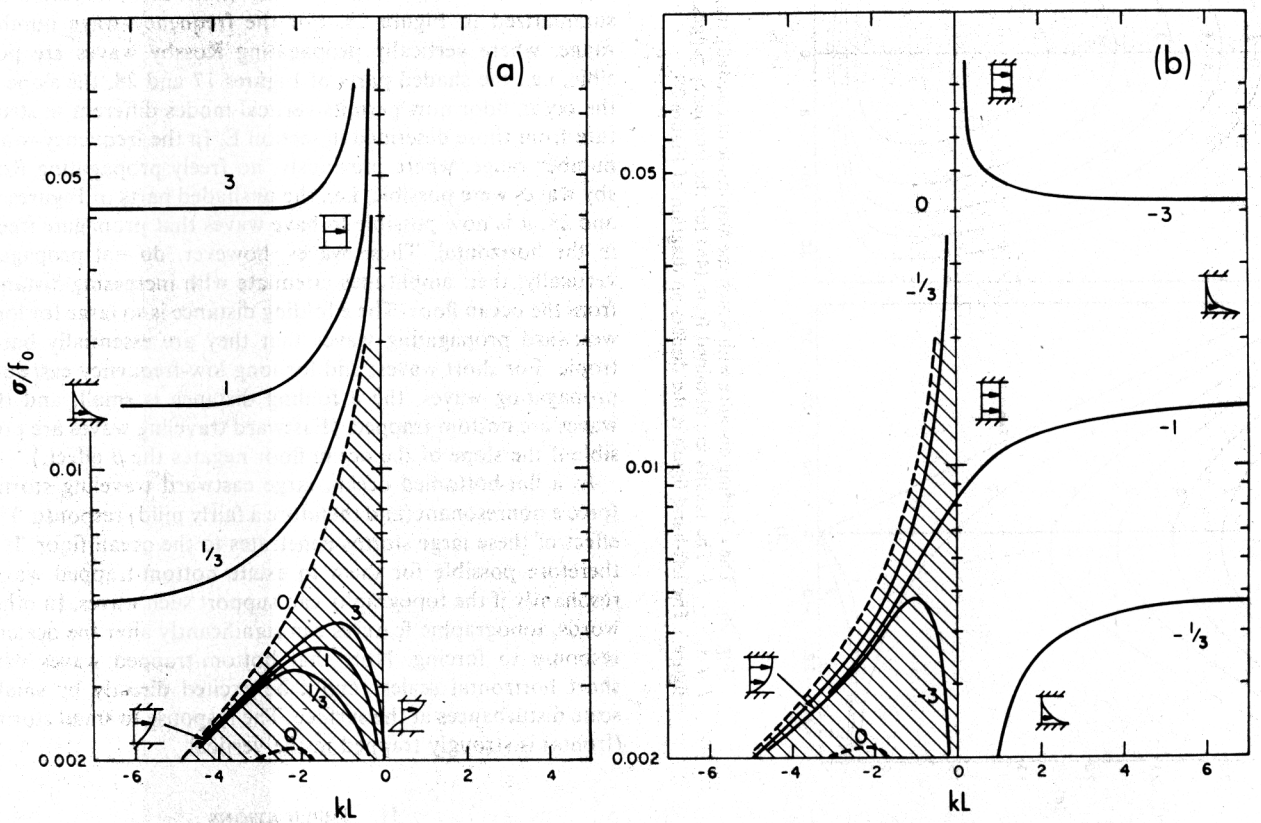

Fig. 28. Dispersion relation for bottom-trapped waves (in the unshaded region) and for 'surface' modes (in the shaded region) as a function of nondimensional frequency (f_0 is the inertial frequency at 43°N) and wave number (L = 120 km) for different values of the slope of the ocean floor (measured in units of $\beta H/f_0$). The insets show the vertical structure of the waves. The dashed curves are Rossby waves (barotropic and first baroclinic mode) in the absence of topography. In Figure 28*a* (Figure 28*b*) the ocean floor slopes upward (downward) toward the poles and thus enhances (competes with) the β effect [after *Rhines*, 1970].

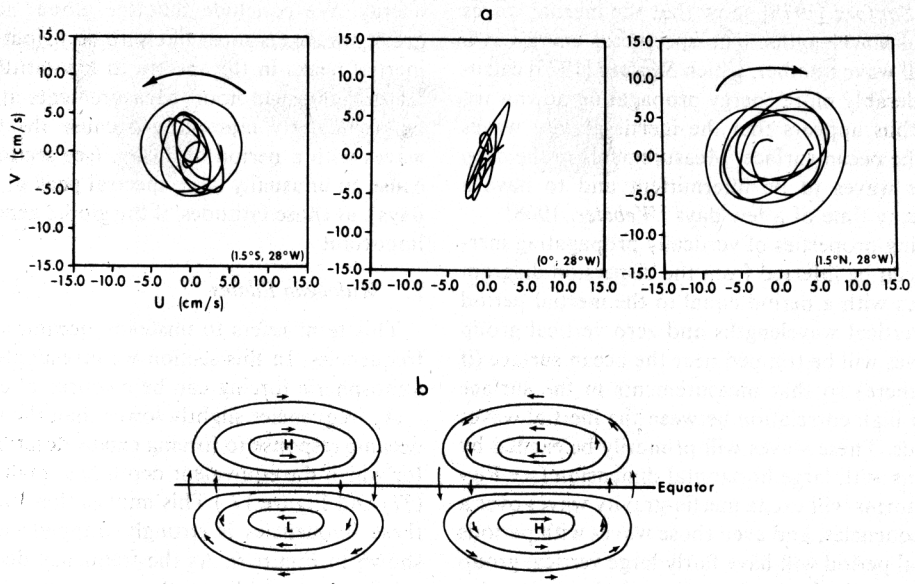

Fig. 29. (*a*) Velocity and pressure distribution in a horizontal plane for Rossby-gravity waves [after *Matsuno*, 1966]. (*b*) Hodographs of the horizontal velocity components associated with a westward propagating Rossby-gravity wave which has a period of 10 days. The measurements were made in the equatorial Atlantic by *Weisberg et al.* [1976] at a depth of 300 m.

waves is about 2½ days. At the lowest resolvable frequencies, on the other hand, the measurements of *Weisberg et al.* [1977] had symmetry properties about the equator; this implies that the gravest latitudinal modes are established at low frequencies. As regards the vertical structure, measurements of velocity fluctuations at different depths on the same mooring show consistent upward phase propagation (and presumably downward energy flux). The measurements in the Atlantic therefore suggest that equatorially trapped waves do exist but that vertically standing modes are not established. The reason for this is presumably the rough bottom topography of the equatorial Atlantic that scatters waves incident on it. The mid-Atlantic ridge passes through the region where the measurements were made. The absence of vertical modes implies that the equator in the Atlantic is not an efficient wave guide for the zonal propagation of energy. (Energy propagates most efficiently away from a localized forced region as a standing vertical mode.)

There is reason to believe that the ocean floor is a better reflector, and the equator a more efficient wave guide, in the Pacific than in the Atlantic. *Wunsch and Gill* [1976] have explained peaks, at 4 and 5.5 days, in sea level spectra from islands in the Pacific Ocean as resonant equatorially trapped first baroclinic mode inertia-gravity waves. According to these authors the modes will be excited even if the spectrum of the atmospheric forcing were white. In that case, waves that have zero zonal group velocity will be the most energetic (because their energy does not disperse). *Wunsch and Gill* [1976] assume that the waves observed in the Pacific satisfy this condition.

Over the Atlantic and Pacific oceans there are atmospheric waves with wavelengths of 2000–3000 km and periods of 3–5 days that propagate westward along the Intertropical Convergence Zone [*Wallace*, 1971; *Burpee*, 1974]. The peaks in the spectra of the surface winds can, for prolonged periods, be sharp at periods of 5 and 4 days. (See the sea surface wind and pressure spectra in the paper by *Wunsch and Gill* [1976].) The question therefore arises whether the 4- and 5.5-day oceanic oscillations are not simply forced by the atmospheric waves. Forcing at a period of 4 days and a wavelength of −3000 km will, according to (28), excite an infinite set of inertia-gravity waves with the following equivalent depths for the gravest modes: $h_l^+ = 190$, 80, and 44 cm. At a period of 5.5 days and a wavelength of −3000 km the corresponding equivalent depths are $h_l^+ = 65$, 30, and 15 cm. (No Rossby waves are excited by these disturbances, but a complete description of the response must include modes for which $h < 0$.) The equivalent depth of the first baroclinic mode for the central Pacific is in the neighborhood of 70 cm. Hence at a period of 4 days the $l = 2$ mode, and at a period of 5.5 days the $l = 1$ mode, could be resonantly excited by the atmospheric waves. These are the modes that *Wunsch and Gill* [1976] fit to the data, but they assert that the zonal wavelength, rather than being determined by the forcing function, corresponds to the zero zonal group velocity point on the dispersion diagram. The nonresonantly forced latitudinal modes, which are disregarded by Wunsch and Gill, will of course also be excited. In the case of the 5.5-day oscillation these other latitudinal modes will have a small effect on the sea level because of their small equivalent depths. In the case of the 4-day wave, however, the $l = 1$ mode may have a significant influence on the sea level (because of its large equivalent depth). It is noteworthy that the agreement between the observed and the calculated structure of the $l = 1$, 5.5-day mode is excellent, but in the case of the $l = 2$, 4-day mode the agreement is not particularly good. Further measurements are necessary to assess the importance of the nonresonant modes. It will be interesting to know whether there are resonant 4- and 5.5-day modes in the Indian Ocean, because in that ocean there are no known atmospheric waves with these periods.

2. *Inertia-Gravity Waves*

Measurements at practically all latitudes (poleward of about 4°N and 4°S) and at all depths in the oceans show evidence of inertial currents that rotate (clockwise in the northern hemisphere) at a rate of 2 sin (latitude) revolutions per day. This motion is associated with a prominent spectral peak at (or very near) the local inertial period. At the ocean surface there is a high correlation between these waves and the winds [*Pollard and Millard*, 1970], but this is not true at greater depths. The

measurements of *Sanford* [1975] show that the inertial waves have short vertical wavelengths. The spectra of energy as a function of vertical wave number, which *Sanford* [1975] calculated, show considerably more energy propagating downward than upward. It thus appears that the inertia-gravity waves have a source at the ocean surface. Measurements in the deep ocean show these waves to be intermittent and to have a generation and decay time of a few days [*Webster*, 1968].

Several interesting properties of vertically propagating inertia-gravity waves can be inferred from the dispersion diagram (Figure 15). Waves with a period equal to the inertial period have very short vertical wavelengths and zero vertical group velocity. Such waves will be trapped near the ocean surface (if they are excited there) so that measurements in the surface layers will show a high correlation between the inertial waves and the local winds. These waves will primarily be excited by atmospheric storms with large horizontal dimension (see Figure 15). Smaller storms will excite inertia-gravity waves over a wider range of frequencies, and even those waves with periods close to the inertial period will have fairly large vertical group velocities. Since they will also have small vertical wavelengths, they will readily propagate across the thermocline into the deep ocean. (*Fomin and Yampolskiy* [1975] describe measurements of waves reflected by sharp gradients in the stratification of the Black Sea.) I. Orlanski (unpublished manuscript, 1970) came to the above conclusions from his study of the local generation of inertia-gravity waves in the ocean. The solutions in that paper show the waves in the deep ocean to be transient. A packet of waves excited at the surface takes of the order of 5 days to reach a depth of 1000 m, and they disappear again after approximately the same period of time. Simultaneous measurements, over a period of several weeks, of the atmospheric conditions and oceanic currents at several depths, are necessary to confirm these predictions.

Locally generated inertia-gravity waves in the deep oceans must, according to Figure 15, have frequencies strictly greater than the inertial frequency. (*Webster* [1968, caption to Figure 4] notes that the spectral peak of one of his near-bottom records is at a period nearly an hour less than the inertial period.) These waves will propagate vertically and horizontally. Latitudinally, they can only go as far as their inertial latitude, where the meridional group velocity will vanish. Waves, with a period equal to the inertial period, in the deep ocean could therefore be due to randomly distributed sources at lower latitudes [*Munk and Phillips*, 1968]. (See also *Kroll* [1974], who uses ray theory to study these waves.) There is no reason why nonlocally generated inertia-gravity waves should have more energy propagating downward than upward. The measurements of *Sanford* [1975] therefore imply that the global generation of these waves is not of great importance in the region where the measurements were made. There may of course be other regions where nonlocally generated waves are important. Figure 3, which shows the characteristics along which the waves propagate, explains why local generation may be important in some regions but not in others. According to this figure the higher the frequency of the waves, the more vertical their characteristics and the larger the number of reflections, at the ocean floor and the ocean surface, between the generation region and the inertial latitude. If the ocean floor is very rough, as it is in the tropical Atlantic, for example, then these waves will be scattered, possibly into shorter waves that will be dissipated. Even under favorable conditions the albedo of the ocean floor cannot be assumed to be 100%, so that a large number of reflections implies a considerable loss of energy. We conclude that the global generation of inertia-gravity waves is most likely to contribute significantly to the inertial peaks in the spectra in low-latitude areas that have a featureless ocean floor. Measurements at 15°N and 15°S will be particularly interesting because the tropical atmospheric waves with a period of 2 days (see section H1 above) should cause an unusually large spectral peak at the inertial period (2 days), at those latitudes, if the global generation mechanism is important.

3. *Midocean Eddies*

This term refers to unsteady oceanic motion at subinertial frequencies. In this section we investigate the extent to which atmospheric forcing can be a source of eddy energy.

At frequencies slightly lower than the inertial frequency the oceanic response to forcing can be described in terms of modes for which the equivalent depth has small negative values. (See (37) and Figure 17.) This implies that the oceanic response at these frequencies is strongly trapped near the surface, as is shown in Figure 6. As the frequency decreases, the values of $-h$ increase rapidly so that energy levels at all depths in the ocean increase with decreasing frequency. (It is assumed that the scale of atmospheric disturbances does not decrease rapidly as the frequency decreases.) This qualitative description of the oceanic spectrum at subinertial frequencies is consistent with measurements. A quantitative comparison, to determine whether predicted energy levels agree with measurements, requires detailed information concerning the spectrum of the forcing function. Such information will also permit an assessment of the role of nonlinear processes. *Thompson* [1971] and *Rhines* [1973] have suggested that the increase in energy levels at depth as the frequency decreases below the inertial frequency may be attributable to a nonlinear (two dimensionally turbulent) cascade of energy from lower frequencies.

Fluctuations in the surface winds in mid-latitudes and high latitudes are most energetic in the frequency band from 2 to 10 days. This range of periods is associated with eastward traveling cyclones (synoptic disturbances) which have a scale of the order of 5000 km [*Willebrand*, 1977; *Byshev and Ivanov*, 1969]. The oceanic response to this forcing can be described in terms of modes for which the equivalent depth has large negative values. (See Figure 17.) It follows that the effect of the forcing will penetrate to the ocean floor (see Figure 6) and that a description in terms of vertically standing modes will require little more than the barotropic and first baroclinic mode. The method of solution outlined in section D gives an estimate of the amplitude of the fluctuations induced by these large atmospheric storms. Let us idealize the situation by assuming a sinusoidal time dependence with a period of 7 days, an east-west scale of +5000 km, and a wind stress amplitude of 1 dyn. If the latitudinal structure of the forcing corresponds to the gravest Hough function for a mid-latitude ocean 5000 km in latitudinal extent, then the oceanic response is practically depth independent and has an amplitude of the order of 2 cm/s. (The flat-bottomed ocean is assumed to be 4 km deep and to have a stratification $N = 4 \times 10^{-3}\ s^{-1}$.)

There have been several measurements that show a correlation between local atmospheric disturbances and velocity fluctuations in the deep ocean: in the Drake Passage [*Baker et al.*, 1977]; along the ridge between Scotland and Iceland in the northern Atlantic (J. Meincke, unpublished manuscript, 1975); and near seamounts east of Bermuda [*Taylor et al.*, 1977]. The depth of penetration of the response to the storms is in accord with the analysis of section D, but the observed amplitudes of

the oceanic fluctuations were often much larger than that calculated above. J. Meincke (unpublished manuscript, 1975), for example, measured speeds of up to 30 cm/s. The most obvious explanation for this discrepancy between the observations and the theory is the neglect of the bottom topography in the analysis of section D. In a flat-bottomed ocean, large energetic eastward traveling storms force the ocean nonresonantly—no free waves are excited—so that the amplitude of the response is relatively small. Should the forcing be in a frequency–wave number range where free waves can be excited, then one expects the response to be more vigorous. The topography of the ocean floor introduces a new class of free waves in a frequency–wave number range where previously, no free waves were possible. (See section G.) The baroclinic topographic waves are trapped near the ocean floor. Hence they are efficiently excited by forcing that penetrates deep into the ocean, such as the forcing by large eastward traveling cyclones in mid-latitudes and high latitudes. It is intriguing that an analysis of hydrographic sections in the Southern Ocean suggests higher levels of eddy energy, and shorter length scales for the eddies, in regions of rough topography than in flat regions (D. J. Baker and J. Lutjeharms, unpublished manuscript, 1977). Further studies of the effect of bottom topography on the forced oceanic response are clearly necessary. At this stage we note that bottom topography will affect both the frequency and the wave number spectra of the oceanic response because the topography will scatter the forced large-scale motion into smaller eddies and because the topography can support a new class of waves.

The large eastward traveling storms in mid-latitudes and high latitudes are the most distinctive features of the atmospheric forcing function. To calculate the oceanic response to forcing at lower frequencies and to determine whether or not Rossby waves are excited, for example, it is necessary to know the frequency and the wave number spectra of the forcing. Information of this type is becoming available now.

4. *Free Waves Excited by Unstable Currents*

Although there has been speculation that even weak currents in the interior of the ocean are baroclinically unstable, only certain intense boundary currents, and some of the zonal equatorial currents, are known to be unstable. These currents are all narrow jets, some of which are confined to the surface layers of the ocean. It is of interest to know whether free waves can radiate energy away, in horizontal and vertical directions, from these geographically small regions of instability. The following remarks are valid if the effects of advection can be neglected in regions distant from the currents.

Inferences concerning the horizontal propagation of nonlocally forced disturbances can be made from Figures 22 and 23. It is evident that barotropic modes with a period of about 1 week or more can readily propagate between high-latitude circles. Baroclinic modes, which have small equivalent depths, can propagate freely in low latitudes only. Thus instabilities of the Florida Current, which have a wavelength of about 120 km and a period of approximately 1 week [*Rao et al.*, 1971], will force baroclinic variability in the oceans that is confined to the immediate neighborhood of this current. Beyond Cape Hatteras, unstable Gulf Stream meanders have a period of about 3 weeks [*Hansen*, 1970], but that is still too short a period for the generation of baroclinic modes that propagate away from the Gulf Stream.

Recent satellite photographs of the sea surface temperature in the central equatorial Pacific show westward propagating undulations, with a wavelength of 1000 km and a period of 25 days, along the front between the cold South Equatorial Current and warm North Equatorial Countercurrent [*Legeckis*, 1977]. These waves are probably due to a shear instability of the above mentioned surface currents. In the deep ocean (below the surface layers) the oscillations will excite vertically propagating equatorially trapped waves. The gravest mode to be excited is a mixed Rossby-gravity wave with an equivalent depth of about 30 cm. Though its phase speed is westward, it has an eastward group velocity. Hence, even though the waves in the surface layers are observed west of 100°W only, fluctuations with a similar period and wavelength are possible in the deep ocean much further east. This is proposed as an explanation for the measurements by *Harvey and Patzert* [1976], who observed oscillations with these scales near the ocean floor near the Galápagos Islands (at 92°W). Despite their long period these 25-day disturbances will not propagate far latitudinally (see Figure 22).

I. Discussion

We have described two representations for the response of the ocean to forcing at a given frequency and zonal wave number. These methods of solution have severe limitations because they involve either vertical or latitudinal modes. For example, neither method is particularly useful in studying the generation of inertia-gravity waves by a mid-latitude atmospheric storm. These waves will have short vertical wavelengths, so the use of vertical modes is inconvenient, and there is obviously little virtue in using equatorially trapped modes to describe the latitudinal structure. Ray theory [see *Kroll*, 1974] offers a more reasonable approach. The methods of solution described here are also inconvenient in solving initial value problems, especially if the time scale of interest is short in comparison with the time that it takes for the vertical or latitudinal modes to become established. In the case of the vertical modes a disturbance has to propagate from the mixed surface layer (where the forcing takes place) to the ocean floor and back to the surface before a standing mode can be said to exist. The manner in which latitudinal modes are established can be inferred from (B14). If we assume that the flow is x independent, then this equation is hyperbolic and has characteristics $y \pm ct$, where $c = (gh)^{1/2}$. Thus in an initial value problem a front propagates poleward from the equator at speed c. Hence the inertia-gravity modes shown in Figure 11 exist only after the front has passed the turning latitude (say) of the modes. (Rossby modes are established in a more complicated manner because x dependence must be retained.) In equatorial regions the gravest latitudinal modes are established rapidly because the north-south extent of the forcing function is comparable to the meridional scale of the modes. The vertical scale of the forcing function, in other words, the depth of the mixed surface layer, is very small in comparison to the depth of the ocean, so the vertical modes take much longer. It is for this reason that we see vertically propagating latitudinal modes in the equatorial oceans.

The modes associated with negative values of h are not solutions of the homogeneous (unforced) equations of motion. It is therefore of no special significance that these modes are trapped at the poles. This merely implies that these modes are more convenient to use in the study of polar regions than in equatorial regions. An oceanic response that is confined to the immediate vicinity of the forcing region is of course possible in equatorial regions. (Consider, for example, x-independent forcing at a low frequency over a narrow latitudinal band

centered on the equator.) It is not practical to describe this response in terms of modes which have their largest amplitude near the poles. However, because these modes are not solutions of the homogeneous equations, one can introduce zonal boundaries at some arbitrary latitude (20°N for the example just cited) and use the $h < 0$ modes that correspond to this zonal channel.

For the solution of initial value problems the method in terms of vertically standing modes has a decided advantage because the depth dependence can be eliminated from the problem without making assumptions about the time dependence. (See (B14).) This method becomes impractical if the oceanic response is trapped near the surface.

The effects of mean currents with horizontal or vertical shears have been neglected in this study, but they could be of considerable importance especially in the tropics, where there are strong surface and subsurface currents. There is good agreement between linear theory and the observed equatorially trapped waves described in section H1, because the phase speeds of the waves greatly exceed those of the currents. More slowly propagating waves could be significantly affected by the currents, particularly so if their phase speeds should equal the current speed at some point. Such critical layers will prevent the establishment of modes. These problems have been studied extensively in the meteorological literature and have been conveniently summarized by *Holton* [1975].

J. SUMMARY

This paper concerns the linear response of the ocean to forcing at a frequency σ and zonal wave number k in the absence of mean currents.

Figure 5 summarizes the importance of different terms in the forcing function as the period and wavelength of the forcing varies: the curl of the wind stress (A) is most important at low frequencies and large scales; pressure fluctuations (E) play a crucial role at small scales and high frequencies, so atmospheric fronts could effectively excite inertia-gravity waves.

The equations of motion are hyperbolic equatorward of the inertial latitudes that correspond to the given frequency σ. In this latitude band, disturbances propagate along characteristics shown in Figure 3. Outside this latitude band the equations are elliptic, and their properties depend on the sign of the quantity

$$q = k^2 + \beta k/\sigma$$

If $q < 0$ (in the shaded parts of Figures 2, 4, and 17), then an unbounded mid-latitude ocean with constant stratification responds to forcing at a point with radiating cylindrical (in y and z) Rossby waves. If $q > 0$ (in the unshaded parts of Figures 2, 4, and 17), then the oceanic response decays exponentially with increasing distance from a point force. Attenuation is most severe at frequencies slightly less than inertial, at high wave numbers, and at very low frequencies for positive values of k.

For a bounded ocean with arbitrary stratification the equations of motion can be solved by a separation of variables. The two equations thus obtained are Laplace's tidal equation for the latitudinal structure (equation (10)) and a vertical structure equation (equations (8) or (16)). LTE can, for certain ranges of the parameters, be simplified considerably by making β plane approximations. The eigenvalues thus obtained agree well with the accurate computations of *Longuet-Higgins* [1968]. The constant of separation, referred to as the equivalent depth h, can be determined from either LTE or the vertical structure equation. Two different mathematical representations of the (unique) solution are therefore possible.

One description of the oceanic response is in terms of its normal modes. The vertical structure of the normal modes is the barotropic and baroclinic modes, which are the eigenfunctions of the homogeneous vertical structure equation and boundary conditions. Tables 1 and 2 give typical values for the equivalent depths (which are always positive). Figure 19 shows typical vertical structures of the eigenfunctions. To solve the forced problem, it is necessary to project the forcing function (which is assumed to be separable) onto the complete set of vertical modes. It then remains to solve an inhomogeneous version of LTE with h specified. This may be done by solving the homogeneous LTE as an eigenvalue problem, the frequency σ being the eigenvalue. The set of latitudinal eigenfunctions thus obtained is complete and can be interpreted as Rossby and inertia-gravity waves. The solution is of course an infinite sum of such eigenfunctions and may not be a wave at all. The solution in terms of the natural vertical modes is convenient if the forcing is nonlocal, because only these modes can propagate into an undisturbed region. The principal result is that it is extremely difficult for baroclinic (but not barotropic) disturbances to propagate horizontally away from the forced region. Instabilities of the Gulf Stream, for example, excite disturbances that are confined to the immediate vicinity of this current; disturbances due to instabilities of equatorial currents do not propagate far latitudinally.

A second description of the oceanic response to forcing is in terms of vertically propagating (or trapped) latitudinal modes. These modes are eigenfunctions of LTE when the eigenvalue is the equivalent depth h (and not the frequency σ as before). For completeness, both positive and negative values of h are necessary. It is evident from (1) that $h > 0$ implies a wavelike vertical structure; $h < 0$ implies an amplitude that attenuates vertically. The $h > 0$ modes fall into two groups: a finite number of Rossby waves if the forcing is such that $q < 0$ and an infinite number of inertia-gravity waves. The gravest modes are equatorially trapped and have been observed in the Atlantic and Pacific. Higher-order inertia-gravity waves have smaller equivalent depths and decay exponentially poleward of their inertial latitude. The higher-order Rossby modes have longer equivalent depths than the gravest modes and extend further poleward. Section D1 concerns the effects of variable stratification on these vertically propagating waves. If $h \sim 1$ cm or less, then the vertical wavelength is so short in regions of high stability (such as the thermocline) that the waves are likely to break or be unstable. At any rate, the establishment of vertically standing modes is unlikely if $h \sim 1$ cm or less. If $h \sim$ 20 cm or more and if the ocean floor is reflective, then vertically standing modes are likely. Internal reflection in strong thermoclines can reduce the role of reflection from the ocean floor in the establishment of the modes. The vertical structure of mid-latitude inertia-gravity waves, which have small values for h, will correspond to vertically propagating waves rather than to standing modes. Mid-latitude Rossby waves, on the other hand, will be in the form of standing modes (unless their frequency is very low). The insets in Figure 17 summarize these mid-latitude results.

Figure 6 shows the effect of variable stratification on $h < 0$ modes. The latitudinal eigenfunctions are exponentially decaying equatorward of a turning latitude so that the gravest of these modes are trapped at the poles. This is not of any physical significance; it merely means that these modes provide a useful description in polar but not equatorial regions (where

an oceanic response that decays exponentially away from the forcing region is also possible). Figure 17 shows the vertical attenuation as a function of the frequency and zonal wave number of the forcing, in mid-latitudes. Of particular interest is the great depth of penetration of forcing due to a series of large-scale eastward traveling cyclones such as the ones that are common in mid-latitudes and high latitudes.

The effect of meridional coasts depends on the frequency. For frequencies close to σ_0 as defined in (55) (see Table 2 for numerical values), the coasts reflect a finite number of equatorially trapped waves (possibly none) which decay exponentially poleward of a latitude y_T, which is defined in (50). Poleward of y_T the only effect of the coast is to introduce coastally trapped Kelvin waves. Their e folding distance from the coast is the radius of deformation. At frequencies much lower than σ_0 the coasts reflect the nearly nondivergent Rossby waves as Rossby waves, and coastal Kelvin waves are unimportant. At frequencies much higher than σ_0, nearly irrotational inertia-gravity waves are reflected as inertia-gravity waves, and coastal Kelvin waves are again unimportant.

The topography of the ocean floor introduces waves that propagate freely in the horizontal in a frequency–wave number range where no free waves are possible if the ocean floor is flat. These topographic waves have amplitudes that attenuate with increasing distance from the ocean floor. They can therefore be excited only by a forcing that penetrates to the ocean floor. It follows that the oceanic response to large eastward traveling cyclones in mid-latitudes and high latitudes can be drastically altered by the topography of the ocean floor.

APPENDIX A: HERMITE FUNCTIONS

The equation

$$\psi_{yy} + (2\nu + 1 - y^2)\psi = 0$$

has solutions that are bounded at large values of y only if ν is an integer. These solutions can be written

$$\psi = (-1)^\nu e^{y^2} \frac{d^\nu}{dy^\nu}(e^{-y^2}) \equiv e^{(1/2)y^2} G_\nu(y)$$

$$G_0 = 1 \qquad G_1 = 2y \qquad G_2 = 4y^2 - 2$$
$$G_3 = 8y^3 - 12y \qquad G_4 = 16y^4 - 48y^2 + 12 \tag{A1}$$
$$G_5 = 32y^5 - 160y^3 + 120y$$

Note that

$$(d/dy)G_\nu = 2\nu G_{\nu-1} \tag{A2}$$

$$yG_\nu = \nu G_{\nu-1} + \tfrac{1}{2}G_{\nu+1} \tag{A3}$$

$$\int_{-\infty}^{\infty} G_m\, G_n\, e^{-y^2}\, dy = \delta_{mn}\, 2^n n! \pi^{1/2} \tag{A4}$$

APPENDIX B: APPROXIMATIONS TO LAPLACE'S TIDAL EQUATIONS

Laplace's tidal equation for pressure perturbations is

$$L(P) - \epsilon P = 0 \tag{B1}$$

where

$$L = \frac{1}{\lambda \sin\theta}\left\{\frac{\partial}{\partial\theta}\left[\frac{1}{\lambda^2 - \cos^2\theta}\left(s\cos\theta - \lambda \sin\theta \frac{\partial}{\partial\theta}\right)\right] + \frac{s}{\lambda^2 - \cos^2\theta}\left(\frac{\lambda s}{\sin\theta} - \cos\theta\frac{\partial}{\partial\theta}\right)\right\}$$

An equivalent equation, but for the meridional velocity component, is

$$\left[(\lambda\nabla^2 - s) + \epsilon\lambda(\lambda^2 - \mu^3) - \frac{2\epsilon\lambda^2\mu}{s^2 - \epsilon\lambda^2(1-\mu^2)}(\lambda D - s\mu)\right] V^* = 0 \tag{B2}$$

where

$$\mu = \cos\theta \qquad D = (1-\mu^2)(d/d\mu)$$
$$\nabla^2 = \frac{d}{d\mu}D - \frac{s^2}{1-\mu^2} \qquad V^* = iV\sin\theta \tag{B3}$$

A detailed discussion of methods of solution for these equations, and graphs and tables of the eigenfunctions and eigenvalues for a wide range of frequencies σ, equivalent depths ϵ, and wave numbers s or k can be found in the paper by *Longuet-Higgins* [1968]. *Flattery* [1967] has calculated the set of Hough functions and equivalent depths for the cases ($\sigma = 2\Omega$, $s = -2$) and ($\sigma = \Omega$, $s = -1$) that are relevant to atmospheric tides [see *Chapman and Lindzen*, 1970].

If we regard the positive equivalent depth h and zonal wave number s or k as specified, then a series of eigenfrequencies σ_l can be calculated from (B1) or (B2). Let V_l denote the associated eigenfunctions. All these functions are sinusoidal equatorward of a turning latitude and exponentially decaying poleward of that latitude. For large values of ϵ the gravest ($l \sim O(1)$) modes are equatorially trapped, but the higher-order modes ($l \gg 1$) extend further and further poleward. For small values of ϵ the turning latitude of all the modes is close to the poles, and the eigenfunctions are sinusoidal over the entire globe.

If, on the other hand, the values of the frequency and zonal wave number are specified, then a series of eigenvalues ϵ_l can be calculated from (B1) or (B2). For the associated eigenfunctions $\tilde{V}_l$ to form a complete set, both positive and negative values of ϵ_l are necessary. The modes associated with negative values of ϵ are sinusoidal poleward of a turning latitude and exponentially decaying equatorward of that latitude. The opposite is true for the modes associated with positive values of ϵ: they are sinusoidal (exponentially decaying) equatorward (poleward) of a turning latitude. These modes can be subdivided into two groups: an infinite set of inertia-gravity modes for which the turning latitude is the inertial latitude for the frequency under consideration and a finite number of Rossby waves that have turning latitudes that increase as l increases or as ϵ decreases.

For the parameter values for which the modes are either equatorially trapped ($\epsilon \gg 1$ and $l \sim O(1)$) or global ($\epsilon \sim O(1)$ or $l \gg 1$), Laplace's tidal equations can be approximated by simpler equations.

Spheroidal Wave Equation

For small values of ϵ or large values of s, (B2) can be simplified to the spheroidal wave equation

$$[\lambda\nabla^2 - s + \epsilon\lambda(\lambda^2 - \mu^2)]V^* = 0 \tag{B4}$$

This equation is accurate for a description of high-order latitudinal modes that extend into mid-latitudes [*Longuet-Higgins*, 1965]. It can also be used to approximate the gravest latitudinal modes when their equivalent depths are large [*Dickinson*, 1968]. *Kamenkovich and Tsybaneva* [1975] have studied ap-

proximate solutions to (B4). A discussion of the solution to this equation, and tables for the computation of the eigenfunctions and eigenvalues $\{S_n^s(\mu), A_n^s\}$, can be found in the work of *Abramowitz and Stegun* [1965], where further references are given. The spheroidal wave functions S_n^s have exactly $n - s$ zeros so that the index (meridional wave number) l may be identified with $n - s$. For low values of $n - s$ and large values of ϵ, S_n^s can be approximated by the Hermite functions described above. If S_n^s has a turning latitude (where its behavior changes from sinusoidal to exponentially decaying as θ decreases), then its behavior there can be approximated by Airy functions [*Longuet-Higgins*, 1965; *Munk and Phillips*, 1968; *Stewartson and Walton*, 1976].

Write

$$\bar{V} = (\sin\theta)^{1/2} V^* \tag{B4}$$

Then (B2) can be written

$$\frac{d^2\bar{V}}{d\theta^2} - \left[(s^2 - \tfrac{1}{4})\operatorname{cosec}^2\theta + \epsilon\cos^2\theta + \frac{s}{\lambda} - \tfrac{1}{4}\right]\bar{V} = 0$$

The statement made in (52) follows from this equation.

There is one set of parameter values for which (B2) cannot be simplified to (B3), namely,

$$\epsilon\lambda^2 \sim s^2 \qquad \mu \ll 1$$

In this exceptional case the equations have the solution

$$V = i\eta e^{-1/2\eta^2} \tag{B5a}$$

$$U = (2/s)\epsilon^{3/4} e^{-(1/2)\eta^2} \tag{B5b}$$

$$\eta = \epsilon^{1/4}\mu \tag{B5c}$$

$$\lambda = (s/\epsilon^{1/2}) + (s/4\epsilon) + O(\epsilon^{-3/2}) \tag{B5d}$$

This solution corresponds to a Kelvin wave on a sphere [*Longuet-Higgins*, 1968].

The approximations related to the spheroidal wave equation are valid provided $\epsilon/n^2 \sim O(1)$. We next consider further approximations, valid when $\epsilon/n^2 \ll 1$.

Associated Legendre Functions

For high-order latitudinal modes ($l \gg 1$) and any equivalent depth (any value of ϵ) or for small values of ϵ and any value of l we recover the solutions originally discovered by *Hough* [1898; also *Dikii*, 1965]. This limit is relevant to global (as opposed to equatorially trapped) phenomena. It is convenient to introduce a stream function $\bar{\Psi}$ and potential Φ:

$$U = \frac{is}{\sin\theta}\Phi - \frac{\partial\bar{\Psi}}{\partial\theta} \tag{B6a}$$

$$V = -\frac{\partial\Phi}{\partial\theta} - \frac{is}{\sin\theta}\Psi \tag{B6b}$$

The modes with positive equivalent depths fall into two groups. Class I, irrotational inertia-gravity waves, is described by

$$\Phi \sim P_n^{|s|}(\mu) \tag{B7a}$$

$$\Psi = 0 \tag{B7b}$$

$$\sigma = [n(n+1)gh/a]^{1/2} \tag{B7c}$$

Here $P_n^{|s|}(\mu)$ is the associated Legendre polynominal of degree n and order s. Since $dP_n^{|s|}/d\mu$ has $(n - |s| + 1)$ zeros, except when $s = 0$, in which case it has $n - 1$ zeros, we can relate the meridional wave number l to n as follows:

$$l = n - s + 1 \qquad |s| \geq 1 \tag{B8a}$$

$$l = n - 1 \qquad s = 0 \tag{B8b}$$

The dispersion relation (equation (B7c)) agrees with (B5d) because the Kelvin wave simply becomes an inertia-gravity wave when $\epsilon \to 0$. In general, $P_n^{|s|}$ is sinusoidal equatorward of the turning latitude and exponentially decaying poleward of that latitude. For large n this latitude is practically at the poles [*Longuet-Higgins*, 1964].

The other (class II) solutions that can readily be obtained when $\epsilon \to 0$ correspond to Rossby waves:

$$\Phi = 0 \tag{B9a}$$

$$\bar{\Psi} = P_n^{|s|}(\mu) \tag{B9b}$$

$$-\frac{s}{n} = n(n+1) + \epsilon\left[\frac{n^2 - s^2}{(4n^2 - 1)n^2} + \frac{n^2(n+1-s)(n+1+s)}{(2n+1)(2n+3)(n+1)^2}\right] + \cdots \tag{B9c}$$

so that $l = n - |s|$. These nondivergent low-frequency waves have been discussed in detail by *Longuet-Higgins* [1964, 1965]. Figure 2, which has plots of (B9c) for $l - 0$, $l - 1$, $l - 2$, and $l - 3$ in the limit $\epsilon = 0$, shows the maximum frequency, as a function of zonal wave number, for the gravest Rossby modes on a sphere. The curve for the mode $l = 0$ coincides with the expression in (36) if β is evaluated at the equator and if $s \gg 1$.

β Planes

Expand the trigonometric functions in (1) in Taylor series about a reference latitude $\pi/2 - \theta_0$ and write

$$x = a\phi\sin\theta_0 \qquad y = a(\theta - \theta_0) \tag{B10}$$

Then equations (1) can be reduced to the single equation

$$\left(\frac{\partial^2}{\partial x^2} + \frac{\partial^2}{\partial y^2}\right)v_t + \beta v_x + \frac{\partial}{\partial z}\left[\frac{1}{N^2}\frac{\partial}{\partial z}(v_{ttt} + f^2 v_t)\right] = F_2 \tag{B11}$$

where $\beta = 2\Omega\sin\theta_0/a$ and the Coriolis parameter is the following:

In the tropics

$$f = \beta y \tag{B12}$$

Outside the tropics

$$f = 2\Omega\cos\theta_0 + \beta y \equiv f_0 + \beta y \tag{B13}$$

(The validity of these approximations will be discussed shortly.) After separation of variables the horizontal structure is described by the equation

$$(\bar{V}_{xx} + \bar{V}_{yy})_t + \beta\bar{V}_x - \frac{1}{gh}\bar{V}_{ttt} - \frac{f^2}{gh}\bar{V}_t = 0 \tag{B14}$$

or, if we write $\bar{V} = V(y)e^{i(kx - \sigma t)}$, by

$$V_{yy} + \left(\frac{\sigma^2}{gh} - k^2 - \frac{\beta k}{\sigma} - \frac{f^2}{gh}\right)V = 0 \tag{B15}$$

For an equatorial β plane, where $f = \beta y$, this equation can also be derived from (B4) without introducing higher-order

approximations. Thus in the tropics, (B15) is as accurate an approximation to (B2), as is (B4). It provides a very accurate description for equatorially trapped waves (for which ϵ is large).

The mid-latitude β plane with f given by (B13) can also formally be derived from (B3). (There are of course severe restrictions on the latitudinal distances over which the approximations are valid.) Equation (B15) becomes considerably easier to solve if f has a constant value, f_0. There are two limits in which this approximation is justifiable.

1. If we consider low-frequency motion with time and length scales L and T such that

$$\frac{\beta L}{f_0} \ll 1 \qquad \frac{1}{Tf} \ll 1$$

but

$$\beta L/f_0 \sim 1/Tf_0$$

and if we assume that L is comparable to the radius of deformation $L_R = (gh)^{1/2}/f_0$, then (B14) and (B15) simplify to

$$(\bar{V}_{xx} + \bar{V}_{yy})_t + \beta \bar{V}_x - (f_0^2/gh)\bar{V} = 0 \qquad \text{(B16}a\text{)}$$

$$V_{yy} - \left(k^2 + \frac{\beta k}{\sigma} + \frac{f_0^2}{gh}\right)V = 0 \qquad \text{(B16}b\text{)}$$

These quasi-geostrophic approximations, which assume that the zeroth-order flow is nondivergent and in geostrophic balance [*Phillips*, 1963] filter out inertia-gravity waves.

2. If we consider motion with a time scale comparable to the inertial period

$$\frac{1}{Tf} \sim O(1) \qquad \frac{\beta L}{f_0} \ll 1 \qquad L \sim \frac{(gh)^{1/2}}{f_0} \qquad \text{(B17)}$$

then the simplified equations are

$$(V_{xx} + V_{yy})_t - \frac{1}{gh}V_{ttt} - \frac{f_0^2}{gh}V_t = 0 \qquad \text{(B18}a\text{)}$$

and

$$V_{yy} + \left(\frac{\sigma^2}{gh} - k^2 - \frac{f_0^2}{gh}\right)V = 0 \qquad \text{(B18}b\text{)}$$

The Rossby waves have now been filtered from (B14) and (B15).

It is inconsistent to retain all the terms in (B14) and (B15) and also to regard f as a constant (f_0). Such an approximation is sometimes made and is accurate in the high- and low-frequency limits.

NOTATION

a radius of the earth.
f Coriolis parameter, which equals $2\Omega \cos\theta$.
g gravitational acceleration.
h equivalent depth.
H depth of the ocean.
k zonal wave number.
l meridional wave number.
m vertical wave number.
N Brunt-Väisälä frequency.
p pressure.
$s = ak \sin\theta$, which equals nondimensional (spherical) zonal wave numbers.
t time.
(u, v, w) eastward, northward, and upward velocity components.
(x, y, z) eastward, northward, and upward coordinates.
$\beta = (2\Omega/a) \sin\theta$.
$\epsilon = 4\Omega^2a^2/gh$.
θ colatitude.
$\lambda = \sigma/2\Omega$.
$\mu = \cos\theta$.
ρ density.
σ frequency.
τ wind stress vector.
ϕ longitude.
Ω rate of rotation of the earth.

Acknowledgments. During the course of this work I had the benefit of numerous fruitful discussions with P. Ripa. Comments by M. Cane, E. Sarachik, C. Wunsch, and a referee on an earlier version of this paper led to significant improvements. J. Held assisted ably with computations and the preparations of figures. J. Stintsman and P. Tunison provided expert technical assistance. This work was supported through the Geophysical Fluid Dynamics Laboratory, NOAA grant 04-3-022-33.

REFERENCES

Abramowitz, M., and I. A. Stegun (Eds.), *Handbook of Mathematical Functions*, National Bureau of Standards, Washington, D. C., 1965.
Baker, D. J., W. D. Nowlin, and R. D. Pillsbury, Antarctic circumpolar current: Space and time fluctuations in the Drake Passage, submitted to *Nature*, 1977.
Blandford, R., Mixed gravity-Rossby waves in the ocean, *Deep Sea Res., 13*, 941–961, 1966.
Burpee, R. W., Characteristics of North African easterly waves during the summer of 1968 and 1969, *J. Atmos. Sci., 31*, 1556–1570, 1974.
Byshev, V., and Y. Ivanov, The time spectra of some characteristics of the atmosphere above the ocean, *Izv. Acad. Sci. USSR Atmos. Oceanic Phys., 5*, 17–28, 1969.
Cane, M., and E. Sarachik, Forced baroclinic ocean motion, *J. Mar. Res., 34*(4), 629–665, 1976.
Chapman, S., and R. S. Lindzen, *Atmospheric Tides*, 200 pp., D. Reidel, Hingham, Mass., 1970.
Dickinson, R. E., On the exact and approximate linear theory of vertically propagating planetary Rossby waves forced at a spherical lower boundary, *Mon. Weather Rev., 96*, 405–415, 1968.
Dikii, L. A., The terrestial atmosphere as an oscillating system, *Izv. Acad. Sci. USSR Atmos. Oceanic Phys., 1*, 275–286, 1965.
Eliassen, A., and E. Palm, On the transfer of energy in stationary mountain waves, *Geophys. Norveg., 22*(3), 1–22, 1960.
Fieux, M., and H. Stommel, Onset of the Southwest Monsoon over the Arabian Sea from marine reports of surface winds, *Mon. Weather Rev., 105*, 231–236, 1977.
Flattery, T. W., Hough functions, *Tech. Rep. 21*, Dep. of Geophys. Sci., Univ. of Chicago, Chicago, Ill., 1967.
Fomin, L. M., and A. D. Yampolskiy, Vertical structure of inertial motions in the sea, *Oceanology, 15*, 21–30, 1975.
Golitzyn, G. S., and L. A. Dikii, Oscillations of planetary atmospheres as a function of the rotational speed of the planet, *Izv. Acad. Sci. USSR Atmos. Oceanic Phys., 2*, 137–142, 1966.
Hansen, D., Gulf Stream meanders between Cape Hatteras and the Grand Banks, *Deep Sea Res., 17*, 495–511, 1970.
Harvey, R. R., and W. C. Patzert, Deep current measurements suggest long waves in the eastern equatorial Pacific, *Science, 193*, 883–885, 1976.
Holton, J., The dynamic meteorology of the stratosphere and mesosphere, *Meteorol. Monogr., 15*(37), 216 pp., 1975.
Hough, S. S., On the application of harmonic analysis to the dynamical theory of tides, II, On the general integration of Laplace's tidal equations, *Phil. Trans. Roy. Soc. London, Ser. A, 191*, 139–185, 1898.
Kamenkovitch, V. M., and T. B. Tsybaneva, Analysis of Laplace's tidal equations in a shortwave approximation, *Oceanology, 15*, 151–156, 271–278, 1975.
Kato, S., Diurnal atmospheric oscillation, *J. Geophys. Res., 71*(13), 3201–3214, 1966.
Krishnamurti, T. N., C. E., Levy, and H. L. Pan, On simultaneous surges in the trades, *J. Atmos. Sci., 32*, 2367–2370, 1975.

Kroll, J., The propagation of wind-generated inertial oscillations from the surface into the deep ocean, *J. Mar. Res., 33,* 15–51, 1974.

Legeckis, R., Long waves in the eastern equatorial Pacific: A view from a stationary satellite, *Science, 197,* 1179–1181, 1977.

Lighthill, M. J., Dynamic response of the Indian Ocean to the onset of the southwest monsoon, *Phil. Trans. Roy. Soc. London, Ser. A, 265,* 45–92, 1969.

Lindzen, R. S., On the theory of the diurnal tide, *Mon. Weather Rev., 94,* 295–301, 1966.

Lindzen, R. S., Planetary waves on β-planes, *Mon. Weather Rev., 95,* 441–451, 1967.

Longuet-Higgins, M., Planetary waves on a rotating sphere, *Proc. Roy. Soc., Ser. A, 279,* 446–473, 1964.

Longuet-Higgins, M., Planetary waves on a rotating sphere, *Proc. Roy. Soc., Ser. A, 284,* 40–54, 1965.

Longuet-Higgins, M., The eigenfunctions of Laplace's tidal equations over a sphere, *Phil. Trans. Roy. Soc. London, Ser. A, 262,* 511–607, 1968.

Longuet-Higgins, M., and S. Pond, The free oscillations of fluid on a hemisphere bounded by meridians of longitude, *Phil. Trans. Roy. Soc. London, Ser. A, 266,* 193–223, 1970.

Matsuno, T., Quasi-geostrophic motions in equatorial areas, *J. Meteorol. Soc. Jap., 2*(44), 25–43, 1966.

Mied, R. P., and J. P. Dugan, Internal gravity wave reflection by a layered density anomaly, *J. Phys. Oceanogr., 4,* 493–498, 1974.

Miles, J. W., On Laplace's tidal equations, *J. Fluid Mech., 66,* 241–260, 1974.

Miropolskiy, Yu. Z., N. I. Solntseva, and B. N. Filyushkin, On horizontal variability of the Brunt-Väisälä frequency in the ocean, *Oceanology, 15,* 15, 1975.

Moore, D. W., Planetary gravity waves in an equatorial ocean, Ph. D. thesis, Harvard Univ., Cambridge, Mass., 1968.

Moore, D. W., and S. G. H. Philander, Modeling of the tropical oceanic circulation, in *The Sea*, vol. 6, chap. 8, Interscience, New York, 1976.

Moura, A., The eigensolutions of the balance equations over a sphere, Ph.D. thesis, Dep. of Meteorol., Mass. Inst. of Technol., Cambridge, Mass., 1975.

Munk, W., and N. Phillips, Coherence and band structure of inertial motion in the sea, *Rev. Geophys. Space Phys., 6,* 447–472, 1968.

Oort, A., and A. Taylor, On the kinetic energy spectrum near the ground, *Mon. Weather Rev., 97,* 623–636, 1969.

Orlanski, I., and L. Polinsky, Spectral distribution of cloud cover over Africa, submitted to *J. Atmos. Sci.,* 1977.

Philander, S. G. H., The effects of coastal geometry on equatorial waves, *J. Mar. Res., 35,* 509–523, 1977.

Phillips, N., Geostrophic motion, *Rev. Geophys. Space Phys., 1,* 123–176, 1963.

Pollard, R. T., and R. C. Millard, Comparison between observed and simulated wind-generated inertial oscillations, *Deep Sea Res., 17,* 813–822, 1970.

Rao, P. K., A. E. Strong, and R. Koffler, Gulf Stream meanders and eddies as seen in satellite infrared imagery, *J. Phys. Oceanogr., 1,* 237–239, 1971.

Rhines, P. R., Edge, bottom and Rossby waves in a rotating stratified fluid, *Geophys. Fluid Dyn., 1,* 273–342, 1970.

Rhines, P. R., Observations of the energy-containing oceanic eddies, and theoretical models of waves and turbulence, *Boundary Layer Meteorol., 4,* 345–360, 1973.

Sanford, T., Observations of the vertical structure of internal waves, *J. Geophys. Res., 80,* 3861–3871, 1975.

Stewartson, K., and I. Walton, On inertial oscillations in the oceans, *Tellus, 28,* 71–73, 1976.

Swallow, J. C., Ocean circulation, *Sci. Progr., 49,* 281–285, 1961.

Taylor, P. T., L. A. Banchero, C. M. Gordon, and D. Greenewalt, Bottom water movement and the distribution of acoustically transparent sediment around the Gilliss Seamount, New England Seamount chain, *Eos Trans. AGU, 58*(6), 405, 1977.

Thompson, R., Topographic Rossby waves at a site north of the Gulf Stream, *Deep Sea Res., 18,* 1, 1971.

Turner, J. S., *Buoyancy Effects in Fluids,* 367 pp., Cambridge University Press, New York, 1973.

Tyabin, N. I., and B. A. Sleptsov-Shevlevich, On the reality of existence of sporadic large-scale eddy formations in the ocean, Preliminary Scientific Results of GATE, *Rep. 14,* 397 pp., World Meteorol. Organ., Geneva, Switzerland, 1975.

Veronis, G., and H. Stommel, The action of variable wind stresses on a stratified ocean, *J. Mar. Res., 15,* 43, 1956.

Wallace, J. M., Spectral studies of tropospheric wave disturbances in the tropical western Pacific, *Rev. Geophys. Space Phys., 9,* 557–612, 1971.

Webster, F., Observations of inertial-period motions in the deep sea, *Rev. Geophys. Space Phys., 6,* 473–490, 1968.

Weisberg, R., L. Miller, J. Knauss, and A. Horigan, Equatorially trapped waves in the Atlantic Ocean, submitted to *Deep Sea Res.,* 1977.

Willebrand, J., Spatial and temporal scales of surface winds over the North Atlantic and Pacific oceans, submitted to *J. Phys. Oceanogr.,* 1977.

Wunsch, C., Long-period tides, *Rev. Geophys. Space Phys., 5,* 447–475, 1967.

Wunsch, C., and A. E. Gill, Observations of equatorially trapped waves in Pacific sea level variations, *Deep Sea Res., 23,* 371–390, 1976.

(Received March 1, 1977;
accepted August 30, 1977.)